Review of Applied Science and Technology

Volume: 1; Issue: 4
Pages: 98–145

OPTIMIZATION ALGORITHMS FOR ENHANCING HIGH DIMENSIONAL BIOMEDICAL DATA PROCESSING EFFICIENCY

Rifat Chowdhury[1]; Jinnat Ara[2];

[1]. *Master of Business Administration, University of North Alabama, Florence, AL, USA; Email: rifatahmedchow@outlook.com*

[2]. *Master of Science in Applied Mathematics, Noakhali Science and Technology University, Bangladesh; Email: jinnataraprema51@gmail.com*

Doi: 10.63125/2zg6x055

Received: *15 September 2022;* ***Revised:*** *24 October 2022;* ***Accepted:*** *16 November 2022;* ***Published:*** *25 December 2022*

Abstract

High-dimensional biomedical data processing places substantial computational demands on optimization algorithms due to extreme feature dimensionality, sparsity, missingness, and heterogeneous task structures. This study quantitatively evaluated how optimization algorithm families influenced processing efficiency under fixed task-quality constraints across representative biomedical workflows, including predictive modeling, feature selection, and reconstruction tasks. A controlled benchmarking design was applied to 12 high-dimensional datasets, producing 1,680 algorithm executions across 14 algorithm variants and 7 algorithm families, with 10 repeated runs per condition. Processing efficiency was operationalized using multiple indicators, including wall-clock time-to-target, peak memory usage, iterations or epochs to convergence, throughput, and numerical stability outcomes. Descriptive results showed that time-to-target runtime ranged from 2.8 s to 1,420.6 s, with a median of 96.4 s, while peak memory usage ranged from 0.9 GB to 21.6 GB, with a median of 6.3 GB. Constraint failure occurred in 6.8% of runs, and numerical error events were observed in 2.1% of executions. Mixed-effects regression analyses demonstrated statistically significant differences across optimization algorithm families for runtime, memory usage, and convergence behavior after controlling for feature dimensionality, sparsity ratio, missingness rate, and task type. Scaling analysis indicated that increasing feature dimensionality from 10,000 to 250,000 features increased median runtime from 42.3 s to 188.9 s and median peak memory from 3.1 GB to 9.7 GB under constant performance constraints. Reliability analysis supported the internal consistency of the composite efficiency framework, with an overall Cronbach's alpha of 0.89. Overall, the findings demonstrated that optimization algorithm choice produced statistically measurable differences in efficiency, stability, and scalability in high-dimensional biomedical data processing, highlighting the importance of structured, constraint-based benchmarking for robust comparative evaluation.

Keywords

Optimization Algorithms, High-Dimensional Biomedical Data, Computational Efficiency, Scalability, Stability.

INTRODUCTION

High-dimensional biomedical data refers to datasets in which the number of measured variables substantially exceeds or is comparable to the number of observations, resulting in complex data structures characterized by extreme dimensionality, sparsity, and heterogeneity (Mirza et al., 2019). In biomedical contexts, such data commonly emerge from genomics, transcriptomics, proteomics, metabolomics, medical imaging, electrophysiology, wearable biosensors, and large-scale electronic health records. Each observation may contain thousands to millions of features, representing molecular signals, spatial intensities, temporal measurements, or clinical codes. From a quantitative standpoint, high dimensionality fundamentally alters the geometry of data spaces, affects statistical stability, and increases computational burden across all stages of data processing. Processing efficiency in this domain encompasses not only computational speed but also memory utilization, numerical stability, scalability, and the preservation of meaningful biological information under constrained resources (Moon et al., 2019). Optimization algorithms are formally defined as systematic mathematical procedures designed to identify optimal or near-optimal solutions under predefined objective functions and constraints. In high-dimensional biomedical data processing, these algorithms serve as the operational backbone for feature selection, parameter estimation, dimensionality reduction, signal reconstruction, classification, clustering, and model calibration. The international significance of this topic arises from the global scale of biomedical data generation and sharing, including multinational research consortia, cross-border clinical trials, and population-level health surveillance systems. Countries with varying levels of computational infrastructure face common challenges in managing and analyzing high-dimensional biomedical datasets efficiently, making algorithmic optimization a universal concern rather than a localized technical issue. Inefficient processing directly translates into increased analysis time, higher energy consumption, reduced reproducibility, and limited accessibility of advanced analytics in resource-constrained settings (Razzak et al., 2020). Consequently, optimization algorithms are not auxiliary tools but central quantitative mechanisms that determine whether high-dimensional biomedical data can be processed, interpreted, and utilized effectively across diverse international research and healthcare environments.

From a mathematical perspective, optimization algorithms operate by iteratively improving candidate solutions with respect to objective functions that quantify error, likelihood, divergence, or reconstruction fidelity (Houari et al., 2016). In biomedical data processing, these objective functions often incorporate regularization terms to control overfitting, enforce sparsity, or impose structural constraints aligned with biological assumptions. The distinction between convex and nonconvex optimization is particularly consequential in high-dimensional settings, as it influences convergence guarantees, solution uniqueness, and computational tractability. Convex optimization problems allow efficient and predictable solution paths, making them attractive for large-scale biomedical applications where reliability and reproducibility are critical. Nonconvex optimization problems arise frequently in latent-variable models, matrix and tensor factorizations, neural representations, and manifold-based learning, all of which are common in biomedical analytics. In such cases, processing efficiency depends heavily on algorithm design choices, including initialization strategies, step-size control, and stopping criteria (Feldman et al., 2017). Iterative first-order methods reduce computational cost per iteration by relying on gradient information, while second-order and quasi-second-order methods trade increased per-iteration cost for potentially faster convergence. In high-dimensional biomedical contexts, memory constraints often render full second-order methods impractical, elevating the importance of limited-memory and approximate techniques. Optimization efficiency is further influenced by data access patterns, sparsity exploitation, and numerical precision management, particularly when biomedical datasets exceed the capacity of single-machine memory. The quantitative evaluation of optimization algorithms therefore involves a multidimensional efficiency profile that includes runtime complexity, memory footprint, convergence behavior, and robustness to noise (Sompairac et al., 2019). These characteristics determine how effectively biomedical data processing pipelines can operate across institutions with heterogeneous hardware capabilities, reinforcing the global relevance of algorithmic optimization in high-dimensional biomedical analysis.

A major source of inefficiency in high-dimensional biomedical data processing originates from redundant, irrelevant, or weakly informative features that inflate computational cost without

proportionate analytical benefit. Dimensionality reduction and feature selection techniques address this issue by optimizing criteria that preserve essential information while reducing representational complexity (Halilaj et al., 2018; Jinnat & Kamrul, 2021). Linear dimensionality reduction methods formalize this objective by projecting data onto lower-dimensional subspaces that capture maximal variance or covariance structure. Sparse optimization methods extend this concept by explicitly penalizing model complexity, yielding solutions that rely on a limited subset of features. In biomedical applications, sparsity is particularly valuable because it aligns with biological interpretability, such as identifying key genes, biomarkers, or imaging regions associated with specific conditions. The efficiency of these approaches depends not only on the statistical formulation but also on the optimization algorithms used to solve them (Phinyomark et al., 2018; Zulqarnain & Subrato, 2021). Coordinate-wise optimization, proximal methods, and path-following algorithms enable rapid exploration of regularization regimes, significantly reducing computational overhead in high-dimensional regression and classification tasks. Signal reconstruction problems in biomedical imaging and spectroscopy similarly rely on optimization-based sparsity enforcement to reduce data acquisition and processing requirements. Nonlinear dimensionality reduction methods, which seek to preserve local or global geometric relationships, introduce additional optimization challenges due to their complex objective landscapes and reliance on neighborhood computations. Efficient approximate solutions and data structures are therefore essential to maintain tractability at scale (Uddin et al., 2022; Myszczynska et al., 2020). In international biomedical research settings, where datasets are often pooled from multiple sources with varying quality and resolution, dimensionality reduction optimized for efficiency plays a critical role in harmonizing data representations and enabling downstream analysis within feasible computational limits.

Figure 1: Biomedical Data Optimization Efficiency

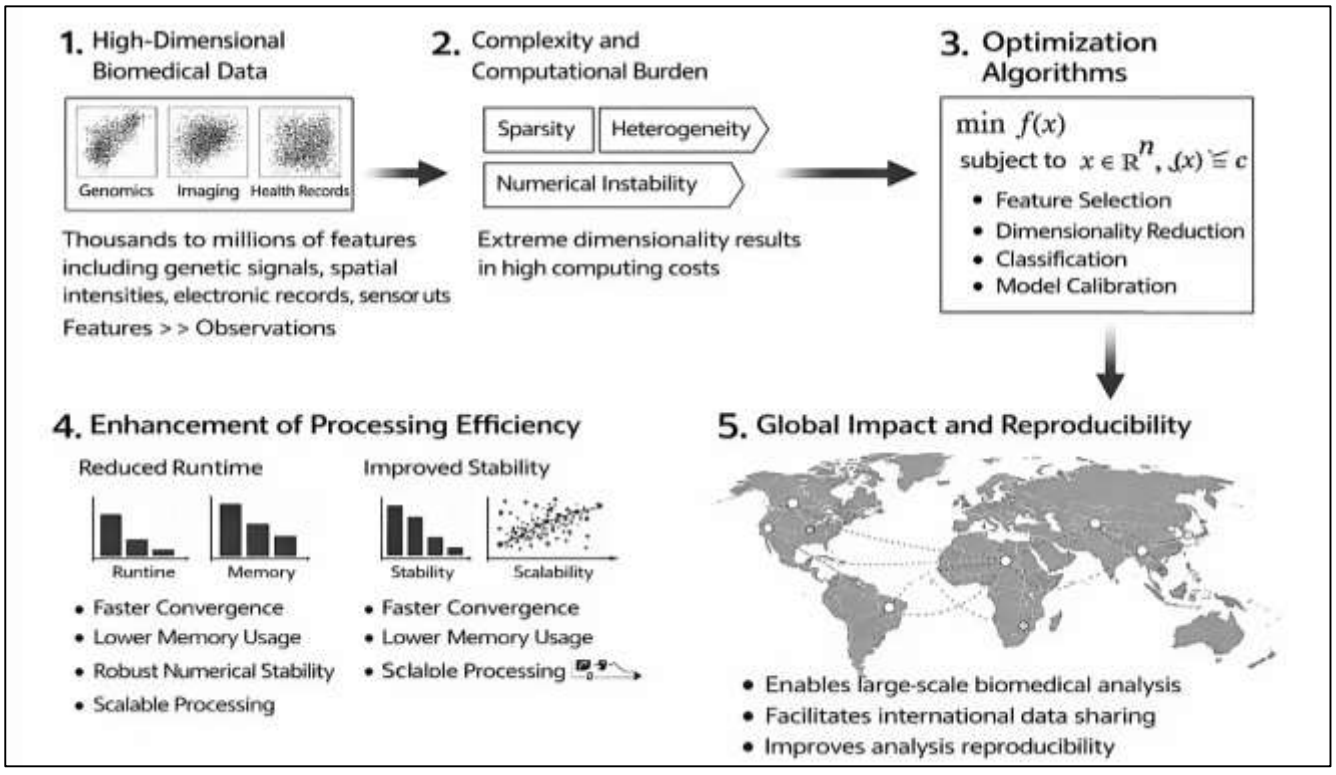

Scalability represents a defining requirement for optimization algorithms applied to high-dimensional biomedical data, particularly when datasets encompass millions of samples or features distributed across institutions and geographic regions (Gao et al., 2018). Large-scale biomedical data processing frequently involves decomposable objective functions, enabling parallel or distributed optimization strategies. Stochastic optimization methods achieve scalability by replacing full-data updates with subsampled approximations, substantially reducing per-iteration cost while maintaining acceptable

convergence properties. These methods are especially effective in settings where data are too large to be processed in a single batch or where data arrive sequentially. Distributed optimization frameworks partition data and computation across multiple nodes, coordinating updates through consensus or dual-variable mechanisms. Such approaches align naturally with biomedical data architectures, where patient records, imaging studies, or molecular profiles can be processed independently before aggregation. Efficiency gains arise from reduced memory contention, improved cache utilization, and parallel execution of linear algebra operations (Akbar & Sharmin, 2022; Tsang et al., 2019). Sparse data representations further enhance scalability by eliminating unnecessary computations on zero-valued entries, which are common in biomedical feature matrices. Ensemble-based learning methods also contribute to scalable optimization by decomposing complex models into collections of simpler components trained on subsets of data or features. The cumulative effect of these strategies is a processing pipeline that remains operational as data dimensionality and volume increase, a requirement that transcends national boundaries as biomedical datasets continue to grow in size and complexity across global research networks (Foysal & Subrato, 2022; Wade et al., 2017).

Figure 2: Optimizing High-Dimensional Biomedical Data

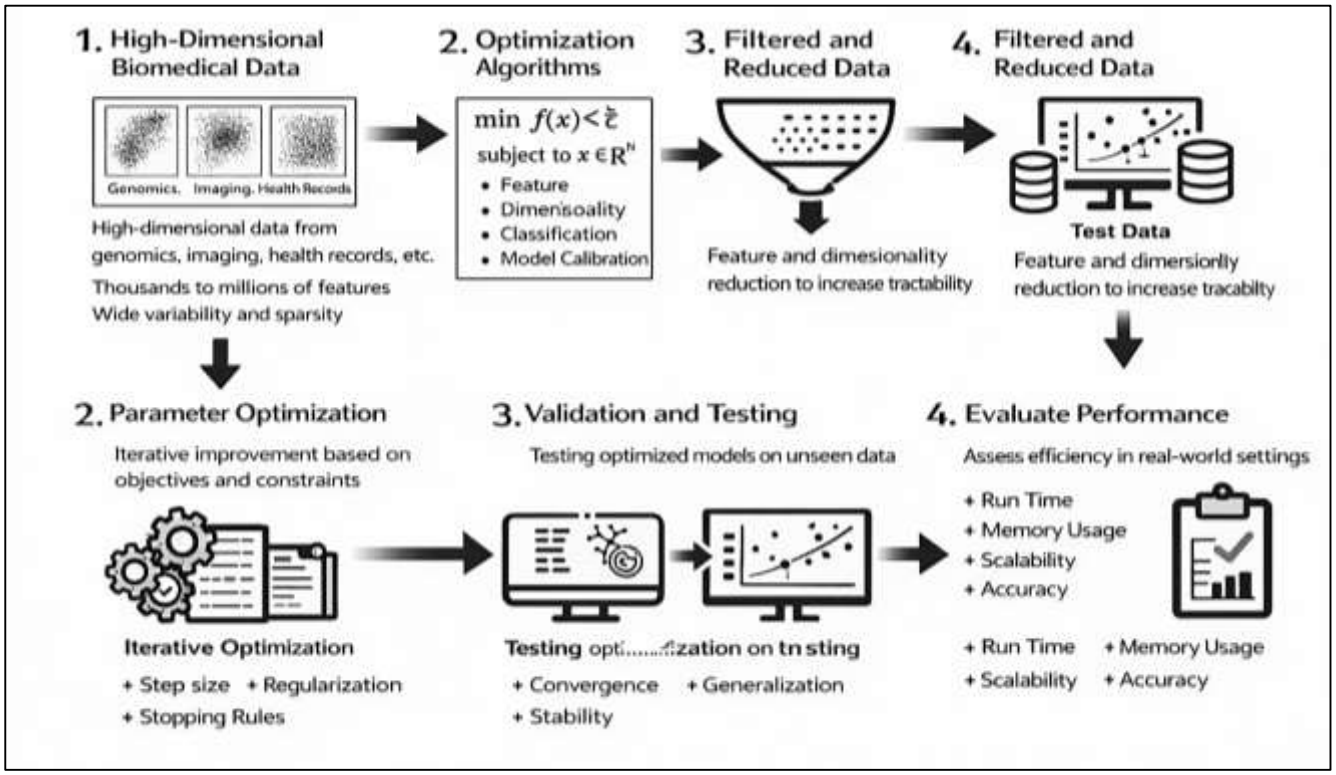

The growing use of nonlinear and highly parameterized models in biomedical analytics places additional demands on optimization algorithms with respect to efficiency. Deep learning architectures, for example, involve optimizing millions of parameters across multiple layers, requiring iterative gradient-based methods that must balance computational cost with numerical stability (Fan et al., 2020). In high-dimensional biomedical imaging, such models process large volumetric data, making memory management and parallelization critical determinants of efficiency. Optimization algorithms employed in these contexts must accommodate noisy gradients, heterogeneous feature scales, and complex loss surfaces while maintaining acceptable throughput. Adaptive optimization methods adjust update magnitudes based on historical gradient information, improving stability in sparse or noisy biomedical data regimes. Momentum-based approaches accelerate convergence by smoothing update trajectories, reducing oscillations that waste computational effort (Zhang et al., 2018). Beyond parameter optimization, hyperparameter tuning introduces a second layer of optimization that significantly affects overall processing efficiency. Biomedical models are sensitive to learning rates, regularization strengths, architectural choices, and preprocessing parameters, each of which can

multiply computational cost if explored exhaustively. Optimization strategies that reduce the number of required evaluations therefore play a central role in efficient biomedical data processing. Population-based and evolutionary optimization methods further expand the algorithmic toolkit by enabling search in complex, non-differentiable spaces where gradient information is unavailable or unreliable. Collectively, these methods demonstrate that optimization efficiency in high-dimensional biomedical contexts encompasses both model fitting and model configuration, reinforcing the need for integrated algorithmic strategies (Landi et al., 2020).

Efficiency in high-dimensional biomedical data processing is also tightly linked to numerical linear algebra and system-level considerations that influence how optimization algorithms are realized in practice (Bote-Curiel et al., 2019; Zulqarnain, 2022). Many biomedical optimization problems require repeated matrix–vector multiplications, eigenvalue computations, or graph-based operations, each of which can dominate runtime if not implemented efficiently. First-order optimization methods reduce computational burden by avoiding explicit matrix inversions or Hessian calculations, making them suitable for large-scale problems. Preconditioning and normalization techniques improve numerical conditioning, reducing the number of iterations required to reach acceptable solutions. Proximal optimization methods further enhance efficiency by transforming complex constrained problems into sequences of simpler subproblems with closed-form solutions (Korsunsky et al., 2019). Limited-memory quasi-Newton methods strike a balance between curvature exploitation and memory constraints, offering improved convergence without prohibitive storage requirements. System-level frameworks for automatic differentiation and parallel execution influence optimization efficiency by determining how computational graphs are constructed and executed. Dataflow scheduling, memory reuse, and kernel fusion directly affect the realized performance of optimization algorithms on modern hardware. In distributed biomedical analytics, communication overhead between compute nodes becomes a critical factor, shaping algorithmic choices regarding synchronization frequency and update aggregation (Shukla et al., 2020). These considerations highlight that optimization efficiency is an emergent property of mathematical formulation, algorithmic design, and computational implementation, all of which must be aligned to process high-dimensional biomedical data effectively at scale.

High-dimensional biomedical data processing increasingly involves integrated analyses that combine multiple data modalities into unified optimization frameworks. Multi-omics integration, imaging–clinical data fusion, and longitudinal patient modeling all introduce additional dimensionality and structural complexity (Ravì et al., 2016). Optimization algorithms address these challenges by incorporating structured constraints such as low-rank representations, graph-based regularization, and multi-task objectives that exploit shared information across data sources. Tensor-based optimization methods organize multiway biomedical data into compact factorized forms, reducing computational cost while preserving relational structure. Graph-structured optimization supports the analysis of biological networks, spatial relationships, and similarity structures, relying on sparse representations and efficient solvers. In large-scale single-cell and population studies, optimization routines are embedded throughout the processing pipeline, from normalization and feature selection to clustering and latent representation learning (Bzdok et al., 2019). Each stage contributes cumulatively to overall efficiency, making algorithmic choices at every step quantitatively significant. Clinical predictive modeling further illustrates the importance of efficient optimization, as high-dimensional feature representations derived from health records must be processed repeatedly across large patient cohorts. Regularized models, ensemble methods, and representation learning techniques all rely on scalable optimization to remain computationally feasible. Across these applications, optimization algorithms function as the unifying mechanism that enables high-dimensional biomedical data to be processed within realistic computational constraints, supporting quantitative analysis across diverse international research and healthcare environments without extending into interpretive or forward-looking domains (Shehu et al., 2016).

The objective of this quantitative study is to systematically evaluate how optimization algorithms can enhance the processing efficiency of high-dimensional biomedical data by reducing computational cost while maintaining rigorous analytical fidelity across common biomedical workflows. High-dimensional biomedical data in this context include feature-rich matrices and tensors generated from

genomics, transcriptomics, proteomics, metabolomics, medical imaging, and large-scale electronic health records, where the number of variables may reach tens of thousands to millions and where sparsity, heterogeneity, and noise are intrinsic properties. The study aims to quantify efficiency gains attributable to optimization algorithm choice by measuring multiple computational outcomes such as total runtime, convergence iterations, memory consumption, throughput (samples processed per unit time), and numerical stability under controlled experimental conditions. A central objective is to compare representative families of optimization methods—such as deterministic first-order approaches, stochastic gradient-based procedures, proximal and splitting methods for constrained objectives, limited-memory quasi-Newton strategies, and selected derivative-free heuristics—within standardized tasks that reflect biomedical processing demands, including dimensionality reduction, sparse feature selection, model parameter estimation, clustering or embedding construction, and reconstruction-oriented inverse problems. Another objective is to determine how data characteristics (dimensionality level, sparsity ratio, batch heterogeneity, missingness patterns, and noise intensity) influence algorithmic efficiency and convergence behavior, using repeatable experimental designs that enable robust statistical comparison. The study further seeks to identify which algorithm–task combinations yield the highest efficiency under fixed performance constraints, where performance is operationalized through task-specific accuracy or fit measures such as classification error, reconstruction error, likelihood-based criteria, or clustering stability metrics, depending on the workflow evaluated. In addition, the study aims to assess scalability by examining how algorithm performance changes as dataset size increases, including stress-testing across varying sample counts and feature counts to characterize empirical time and space complexity. Finally, the study objective includes establishing a reproducible benchmarking framework that supports consistent measurement across algorithms and datasets, enabling transparent comparison and facilitating the selection of optimization approaches best suited for efficient high-dimensional biomedical data processing under realistic computational constraints.

LITERATURE REVIEW

The literature on optimization algorithms for enhancing high-dimensional biomedical data processing efficiency spans multiple research streams that often use different definitions of "efficiency," evaluate algorithms under non-comparable experimental settings, and report performance using inconsistent computational metrics (Viswanath et al., 2017). High-dimensional biomedical data—such as gene expression matrices, single-cell omics, proteomic spectra, radiomic feature sets, and multimodal electronic health record representations—create unique algorithmic demands because computational cost grows rapidly with feature count, data sparsity, modality heterogeneity, and noise. Within this landscape, optimization algorithms function as the computational engine behind core tasks including dimensionality reduction, sparse feature selection, parameter estimation, clustering/embedding, inverse reconstruction, and hyperparameter tuning (Kale & Sonavane, 2020). The literature review therefore needs to synthesize evidence across algorithm families (first-order, second-order, proximal/splitting, stochastic, derivative-free, and hybrid/meta-optimization methods) while explicitly linking algorithmic choices to measurable computational outcomes. For a quantitative study, the review must also emphasize how prior work operationalizes efficiency through runtime, memory footprint, convergence iterations, throughput, energy cost, and scaling behavior as a function of sample size and dimensionality, while simultaneously preserving task-level analytic performance (e.g., prediction accuracy, reconstruction error, clustering validity) (Pes, 2020). This section organizes and critiques existing research by aligning optimization methods with biomedical workflow stages and by highlighting benchmarking practices, dataset characteristics, and evaluation protocols that determine whether reported efficiency gains are generalizable. The goal is to establish a precise foundation for selecting algorithms and computational metrics that can be tested empirically under controlled, reproducible conditions for high-dimensional biomedical processing tasks.

High-Dimensional Biomedical Processing

High-dimensional biomedical data are commonly defined by the dominance of variables relative to observations, the presence of complex feature spaces, and the rapid growth of computational burden as dimensionality increases (Raidou, 2019). In biomedical research, high dimensionality is not limited to gene expression tables; it also appears in proteomic peptide intensities, metabolomic spectral

signatures, radiomic descriptors, histopathology patches, electroencephalography channels, wearable bio signal streams, and richly encoded electronic health records. Across these domains, "high dimensionality" is operationalized in ways that reflect analytical feasibility rather than a single numeric threshold. A frequent characterization is that the number of features overwhelms the number of samples, which increases the risk of unstable estimation and inflates model search spaces. Another common characterization involves settings where features and samples are of comparable scale, creating sensitivity to noise, collinearity, and design-matrix geometry. Ultra-high dimensional settings are also recognized when feature sets become so large that naïve storage and computation become impractical, and where dimensionality reduction or sparsity-inducing constraints become a prerequisite for any downstream task (Gotz et al., 2019). Feature types in biomedical data further complicate the definition of "dimension" because variables may be continuous (e.g., normalized intensities), count-based (e.g., sequencing reads with overdispersion), categorical and sparse (e.g., diagnosis or medication codes), or structured tensors (e.g., multi-channel images and volumetric voxels). The same patient or specimen can therefore be represented by heterogeneous features that differ in scale, distribution, missingness, and measurement error. Data forms reflect these realities: dense matrices dominate in curated omics panels and engineered radiomic features, sparse matrices dominate in single-cell gene expression and health records, graphs emerge from biological networks and neighborhood relationships, sequences appear in genomic or longitudinal data, and tensors represent multiway measurements in imaging and multimodal fusion. Literature on statistical learning and multivariate analysis frames these settings as fundamentally different from low-dimensional inference because correlation structures, distance measures, and regularization behavior change as dimensionality increases, requiring specialized representations and carefully constrained estimation procedures (Abdullah et al., 2020). Work on sparse modeling, high-dimensional regression, and large-scale machine learning has emphasized that high dimensionality is both a statistical condition and a computational condition, where feasibility depends on the interaction between data structure, algorithm choice, and available compute resources.

Figure 3: High-Dimensional Biomedical Data Workflow

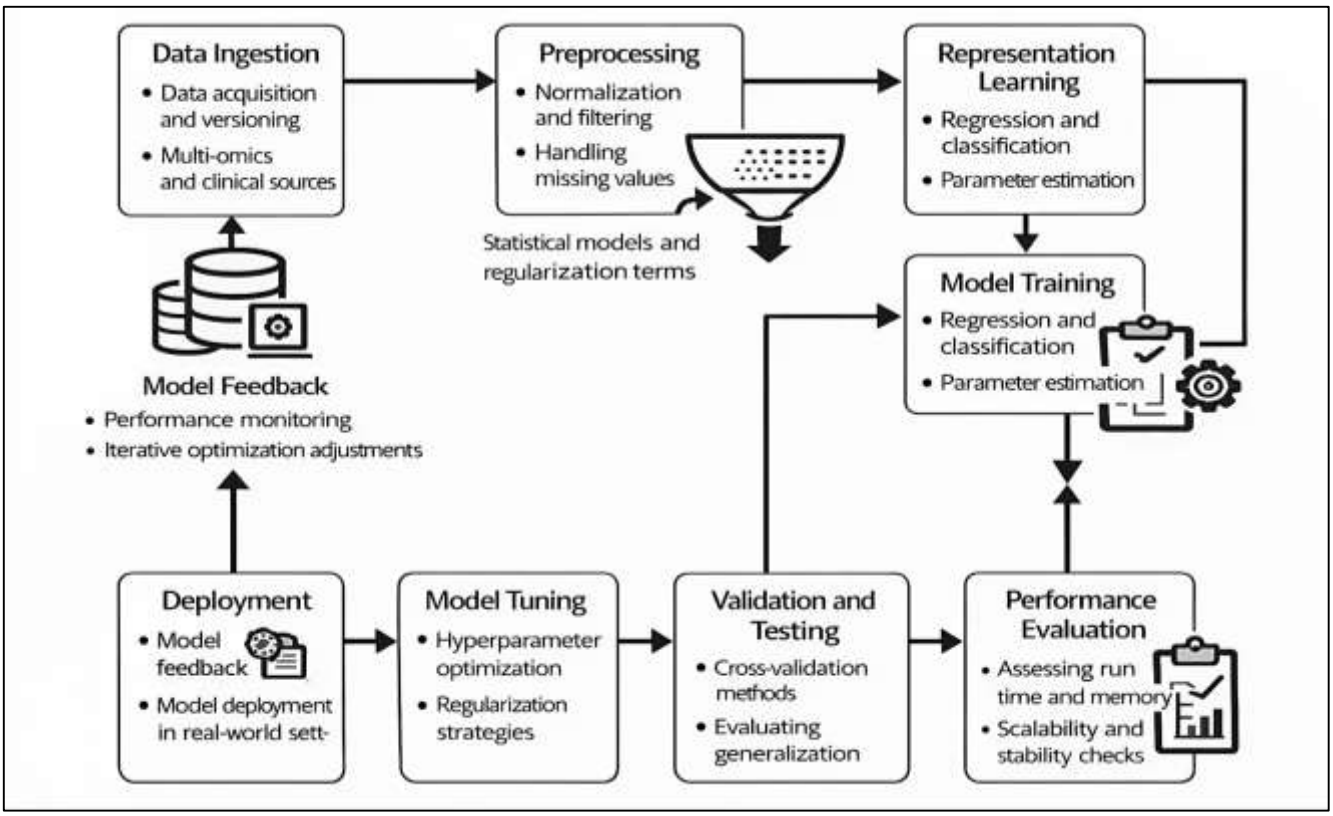

Processing efficiency in high-dimensional biomedical analysis is defined in quantitative terms through explicitly measurable computational outcomes that capture both time and resource consumption under standardized performance constraints (Tseytlin et al., 2016). Runtime is typically treated as a primary indicator, yet the literature differentiates among wall-clock time, CPU time, and accelerator-based time because each reflects a different bottleneck profile. Wall-clock time incorporates system overhead, data loading, and scheduling delays; CPU time reflects core arithmetic and threading efficiency; GPU time captures parallel throughput yet can obscure data-transfer costs. Memory footprint is similarly central because high-dimensional matrices and intermediate tensors can exceed available RAM or device memory, forcing disk spillover, repeated I/O, and degraded performance. Many studies therefore emphasize peak memory usage and memory-access patterns as determinants of feasibility, particularly for sparse biomedical matrices where compressed storage and sparse kernels are needed to avoid dense expansion. Convergence behavior is another major dimension of efficiency because iterative solvers dominate optimization in modern biomedical pipelines; thus, the number of iterations or epochs and the time required to reach a defined tolerance provide a more interpretable basis for comparison than raw runtime alone (Choi, 2018). Throughput complements these measures by reporting processed samples per second or processed features per second, which supports scaling comparisons across datasets of different sizes. Numerical stability indicators are essential because high-dimensional biomedical data can induce ill-conditioning, extreme gradient magnitudes, and floating-point overflow or underflow; many empirical studies therefore track failure modes such as non-finite values, exploding gradients, or unstable step dynamics as part of the efficiency profile. Scaling rates are treated as a summary of computational behavior by examining how time and memory change as sample size, feature size, or sparsity level increases (Raghu et al., 2018). This scaling perspective is widely emphasized in research on convex optimization, stochastic optimization, sparse learning, and large-scale model training because it links algorithm design to expected behavior under realistic biomedical growth patterns. Across machine learning systems research and applied biomedical modeling, efficiency reporting is increasingly framed as a multidimensional scorecard rather than a single number, since an algorithm can be fast yet memory-heavy, stable yet slow, or scalable in samples yet fragile in feature growth (He et al., 2016). Efficiency is therefore interpreted as a balance among runtime, memory, convergence speed, throughput, stability, and scaling behavior, all measured under controlled conditions that define acceptable analytic performance for the task at hand.

A workflow-based mapping clarifies where optimization algorithms affect efficiency in high-dimensional biomedical processing, because optimization is not confined to model fitting; it is embedded throughout the pipeline from raw data to validated outputs (Holzinger, 2019). In preprocessing, optimization appears in normalization and scaling procedures that align distributions across samples, in correction routines that adjust systematic bias, and in filtering or thresholding processes that reduce noise and computational load. Many pipelines treat imputation as an optimization problem, using low-rank structure, neighborhood reconstruction, or regularized estimation to infer missing values without amplifying measurement error. Representation learning forms the second major stage where optimization is explicit: dimensionality reduction, factorization, embedding construction, and manifold-based mapping typically require iterative minimization of reconstruction loss, divergence objectives, or neighborhood-preservation criteria (Lan et al., 2018). High-dimensional biomedical data frequently require sparse or structured representations, making proximal methods, coordinate-wise updates, and constrained optimization frameworks central to achieving tractable embeddings. In modeling, optimization is most visible in parameter estimation for regression and classification, in fitting probabilistic models, in training neural architectures, and in calibrating decision thresholds. Here, efficiency is shaped by the algorithm's update rule, batching strategy, and ability to exploit sparsity, as well as by how the objective combines data fidelity with regularization. Validation introduces additional optimization burdens that are sometimes under-reported in biomedical studies: cross-validation repeats training multiple times; hyperparameter selection becomes a nested optimization process; and threshold selection or calibration can introduce further search procedures. This workflow map also clarifies that the dominant cost center can shift across tasks: for some datasets, neighbor graph construction or feature screening dominates; for others, repeated training runs or reconstruction optimization dominates (Hund et al., 2016). Research across

biomedical machine learning and optimization has repeatedly shown that pipeline efficiency is a cumulative result of many interconnected optimization subproblems rather than a single solver choice. As a result, comparing algorithms meaningfully requires aligning pipeline stages, controlling data preparation costs, and measuring efficiency in a way that accounts for preprocessing, representation learning, modeling, and validation together, rather than isolating only the final model fit.

The scope of high-dimensional biomedical processing is international and cross-institutional because large datasets are generated, shared, and analyzed across multicenter trials, population cohorts, hospital systems, and consortium-based omics and imaging initiatives. This broader scope amplifies the importance of consistent definitions and measurement protocols, since efficiency claims derived from one environment may not generalize to another if hardware, data governance, or storage architecture differ (Krueger et al., 2019). Literature spanning statistical learning, optimization, and biomedical informatics emphasizes that high-dimensional processing problems are shaped by heterogeneity in data acquisition and formatting, including differing measurement platforms, site-specific coding conventions, and variable levels of missingness. These conditions influence both the structure of the optimization problem and the computational behavior of candidate algorithms. Dense imaging tensors and sparse clinical codes, for example, stress very different parts of the compute stack, making the selection of representations and solvers a central determinant of feasibility. Studies on convex optimization and distributed learning highlight that algorithm performance depends on the interplay among objective geometry, conditioning, and data access patterns, while work on large-scale machine learning systems shows that realized efficiency is limited by memory bandwidth, I/O throughput, and communication overhead in distributed settings. Within biomedical contexts, this means that an optimization method cannot be evaluated solely by theoretical iteration complexity; it must be assessed by end-to-end costs that include data loading, preprocessing transforms, iterative updates, and validation repetition (Pandey, 2016). Research on sparse modeling and regularization demonstrates that structural assumptions such as sparsity and low rank can reduce computation by shrinking the effective dimension, yet these benefits depend on solver implementation and stopping criteria. Work on stochastic optimization emphasizes that subsampling reduces per-update cost, yet variance and stability properties affect total time-to-tolerance, especially in noisy biomedical regimes. Systems research further indicates that performance profiles differ across CPU-based and accelerator-based execution, requiring explicit measurement of wall-clock time, memory peaks, and failure modes to compare algorithms fairly. Across these streams, a literature review grounded in conceptual foundations must therefore connect (a) how high dimensionality is defined across biomedical modalities, (b) how efficiency is measured using observable computational metrics, and (c) where optimization appears throughout the biomedical workflow as a sequence of interdependent subproblems, each contributing to the overall processing efficiency profile (Wójcik & Kurdziel, 2019).

Optimization Problem in Biomedical Data Efficiency Studies

Biomedical data efficiency studies typically begin by translating scientific goals into loss functions that are computable, comparable, and sensitive to the types of errors that matter in biomedical decision-making (Huang et al., 2016). Across the literature, loss functions are described as the mathematical "scorecards" that guide optimization, and the selected loss strongly determines computational workload in high-dimensional settings. For continuous biomedical outcomes, regression-oriented losses are often preferred because they are straightforward to evaluate and align well with large-scale linear algebra operations; however, high dimensionality introduces instability through collinearity, heterogeneous scaling, and heavy-tailed noise that can increase iterations and degrade numerical conditioning. For discrete outcomes such as diagnosis categories, treatment response labels, or event occurrence, classification-oriented losses are used to encode separation or probability calibration, and these losses tend to require iterative optimization with careful step control in imbalanced biomedical datasets. Likelihood-based objectives are widely reported in probabilistic biomedical modeling because they unify prediction with uncertainty representation and allow modeling of measurement noise, missingness mechanisms, and latent biological structure (Crown et al., 2017). At the same time, likelihood objectives can be computationally expensive when they include latent variables, normalization terms, or complex link functions that must be evaluated repeatedly. In biomedical imaging and physiological signal processing, reconstruction-based objectives dominate because they

quantify how closely a recovered image or signal matches observed measurements under physical acquisition constraints. These objectives often impose significant computational cost because each iteration may require repeated forward and inverse operators, convolution-like transforms, or repeated evaluations across large voxels, pixels, or time points. Another family of objectives emphasizes distribution alignment and batch harmonization, where the loss is defined not by individual prediction errors but by mismatch between distributions across sites, instruments, or batches. Such distributional objectives can raise computational demand by requiring global statistics, pairwise comparisons, kernel-like operations, or adversarial-style updates that are inherently iterative. The literature therefore treats loss selection as a key driver of efficiency: losses differ in smoothness, curvature, and sensitivity to extreme values, and those properties affect step-size stability, iteration counts, and the likelihood of numerical failures (Albuquerque et al., 2020). In high-dimensional biomedical processing, loss functions are not only scientific statements about what "error" means; they are computational commitments that shape runtime, memory use, convergence speed, and stability across the entire pipeline.

Figure 4: Biomedical Optimization Loss Framework

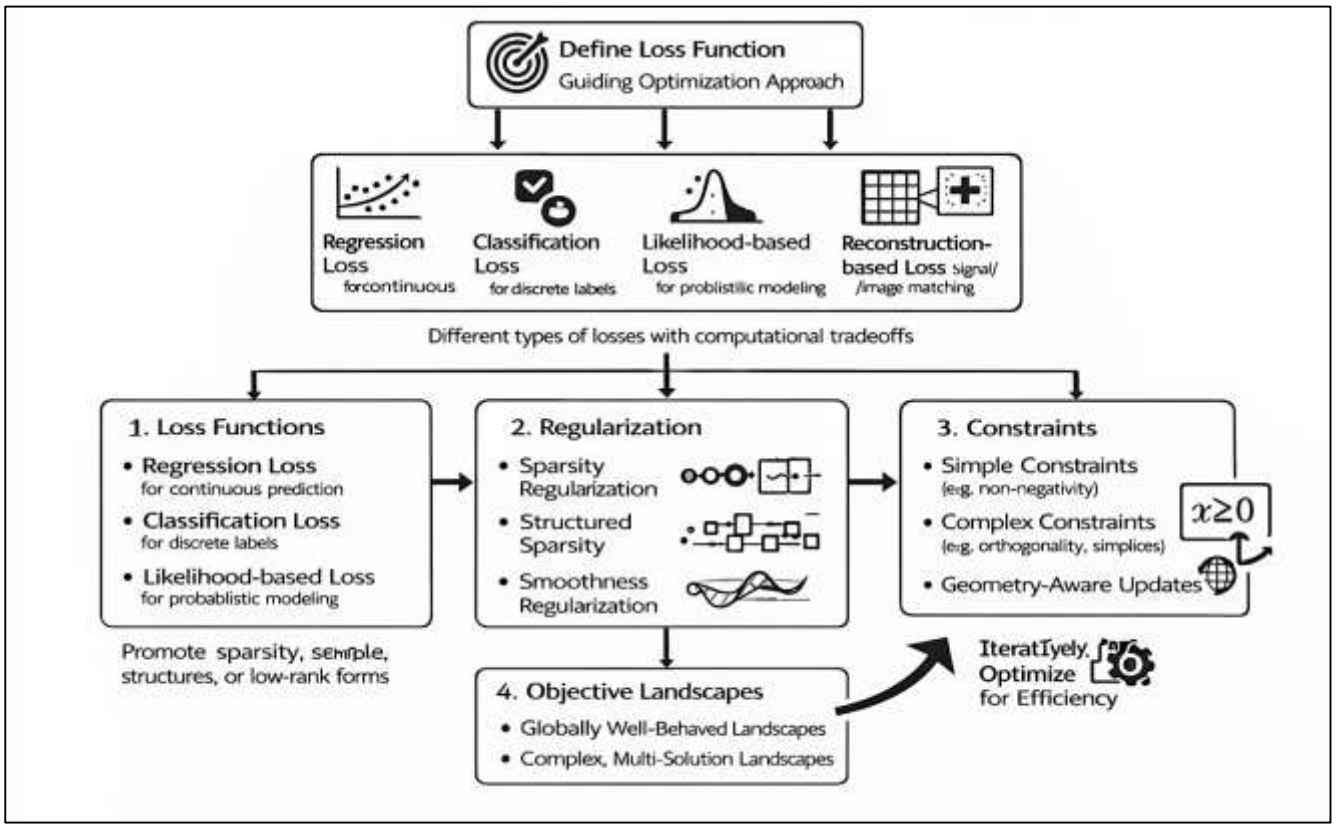

A second dominant theme in efficiency-focused biomedical optimization research is the use of regularization structures to control high dimensionality by shaping solutions toward parsimonious, stable, and computationally manageable forms. Regularization is widely framed as a dual-purpose mechanism: it mitigates overfitting and also reduces computational load by shrinking the effective complexity of the model or representation (Zhou et al., 2016). Sparsity-promoting regularization is particularly prominent because high-dimensional biomedical data often contain many weak or redundant signals alongside a smaller set of informative markers. The literature commonly reports that sparsity reduces computation in two ways: it simplifies the fitted model so inference is faster, and it enables algorithms that operate efficiently on sparse data structures without expanding them into dense forms. Structured sparsity extends this by grouping features according to biological pathways, anatomical regions, or network neighborhoods, which improves interpretability while also constraining the solution space. These structured approaches often increase per-iteration overhead because updates become coupled across feature groups, yet they can reduce total runtime by lowering

dimensionality more aggressively and stabilizing convergence. Smoothness regularization appears frequently in imaging and signal settings, where solutions are encouraged to vary gradually across space or time to suppress noise while preserving meaningful boundaries (De Groote et al., 2016). Edge-preserving and variation-limiting regularization is widely discussed as a way to improve robustness, though it often introduces no smoothness that requires specialized optimization steps and can increase iteration cost unless efficient splitting or proximal updates are used. Low-rank regularization is another recurring strategy in high-dimensional biomedical analysis, especially for multi-omics matrices, imaging stacks, or multimodal fusion problems, where underlying biological processes are assumed to be governed by a smaller number of latent factors. Low-rank structure can substantially reduce storage and computation by representing large arrays through compact factors, but the literature also notes that factorization introduces iterative alternating updates and repeated matrix multiplications that can dominate runtime at scale. Mixed regularization—combining sparsity with low-rank structure appears in studies where data exhibit both localized biomarkers and global latent organization. These mixed formulations often provide strong dimensional control, yet they increase computational complexity because multiple structural components must be balanced and solved jointly (Ulu et al., 2016). Overall, the literature positions regularization as the central tool that converts high-dimensional biomedical problems into solvable ones, with efficiency determined not only by the regularize itself but by solver compatibility, data sparsity, stopping rules, and the cost of evaluating regularized objectives repeatedly.

Biomedical efficiency studies also emphasize that constraints embedded in optimization formulations directly influence solver selection and computational cost, often determining whether a problem is tractable at all under high dimensionality (Cirillo & Valencia, 2019). Constraints are typically categorized as simple or complex based on whether they can be handled through cheap projections or require geometry-aware updates. Simple constraints, such as nonnegativity or bounded parameter ranges, occur frequently in biomedical factor models, interpretable decompositions, probability-like parameterizations, and physically plausible reconstructions. The literature often characterizes these constraints as efficiency-friendly because they enable fast projection steps that are easy to compute and stable across iterations. For example, enforcing nonnegativity can be implemented by thresholding operations that add minimal overhead while encouraging representations that align with nonnegative biomedical quantities such as intensities or counts. Bounded constraints can stabilize training by preventing extreme values that lead to overflow or unstable gradients, indirectly improving runtime by avoiding divergence and restarts. In contrast, complex constraints such as orthogonality, manifold structure, and simplex-type restrictions can impose significant per-iteration costs. Orthogonality constraints, used in certain factorization and representation learning problems, require repeated normalization or re-orthogonalization steps that become expensive as dimensionality grows (Das & Ni, 2017). Manifold constraints appear in embedding, alignment, and structured representation problems where parameters must remain on curved spaces; these constraints require specialized update rules that can slow each iteration and complicate convergence monitoring. Simplex constraints, common in mixture-style representations and constrained clustering, often require repeated normalization and careful numerical handling to maintain feasibility, especially in sparse high-dimensional settings. The literature also highlights those constraints change the computational bottleneck: projection-heavy methods may become memory-bound, while geometry-aware methods may become compute-bound. Constraints influence not only arithmetic cost but also parallelization potential, since some global constraints require coordination across parameters that limits independent updates. As a result, many studies treat constraint design as a fundamental efficiency decision: constraints can stabilize solutions and encode biomedical plausibility, yet they can also increase iteration time, memory movement, and solver complexity (Beykal et al., 2018). Efficiency-focused comparisons therefore tend to report how constraint handling affects time-to-tolerance, peak memory usage, feasibility violations, and numerical stability indicators, making constraints a core element of optimization problem formulation rather than a peripheral modeling detail.

A final organizing axis across biomedical optimization efficiency studies is the distinction between objectives with globally well-behaved landscapes and objectives with complex, multi-solution landscapes, because this difference shapes convergence reliability and the total compute required to

obtain stable results. When an objective landscape supports consistent progress toward a single best solution under standard conditions, efficiency studies often report predictable time-to-tolerance, interpretable stopping criteria, and strong reproducibility across random seeds and hardware environments (Wang et al., 2016). Such landscapes are often favored in high-dimensional biomedical feature selection and risk modeling because they allow standardized benchmarking across datasets and enable fair comparison of runtime, memory footprint, and iteration counts. In contrast, complex landscapes are prevalent in nonlinear representation learning, factorization with coupled constraints, and deep learning models used for imaging, sequence modeling, or multimodal fusion. In these settings, efficiency is frequently dominated by factors that extend beyond the nominal algorithm choice, including initialization quality, sensitivity to step sizes, and susceptibility to unstable updates. The literature repeatedly notes that initialization can amplify compute requirements because poor starting points increase training time, trigger divergence, or lead to solutions that require retraining or additional regularization to stabilize. Iterative methods used in complex landscapes can progress quickly per step but still require many steps to achieve stable performance, particularly when gradients are noisy or when high-dimensional data contain strong heterogeneity across samples and batches (Pham et al., 2020). Many studies also describe how the same objective can behave differently depending on data scaling, sparsity patterns, and noise distribution, meaning that computational efficiency is not a fixed property of an optimizer but an interaction between optimizer dynamics and data geometry. Another recurring theme is that practical performance constraints—such as minimum acceptable accuracy, reconstruction fidelity, or clustering consistency—change the efficiency evaluation: a method that reaches a weak solution quickly may not satisfy performance thresholds, while a slower method may reach the required tolerance with fewer restarts and fewer numerical failures. Therefore, the literature treats landscape complexity as an efficiency determinant because it governs convergence guarantees, sensitivity to hyperparameters, and the frequency of repeated runs needed to obtain stable results. In high-dimensional biomedical processing pipelines, this distinction affects benchmarking design: studies that compare algorithms often emphasize standardized initialization protocols, fixed compute budgets, consistent stopping rules, and multi-run averaging to ensure that measured efficiency reflects algorithmic behavior rather than uncontrolled variability from complex optimization landscapes (Alber et al., 2019).

Algorithm in High-Dimensional Biomedical Tasks

Deterministic first-order methods are repeatedly emphasized in the literature as foundational tools for improving efficiency in high-dimensional biomedical tasks because they rely on inexpensive gradient information and generally require modest memory overhead (Hu et al., 2016). Within biomedical pipelines, deterministic gradient-based variants are frequently used when objectives are smooth and data access is predictable, such as in regularized regression, calibration layers for predictive models, and certain reconstruction subproblems where gradients can be computed efficiently. Coordinate descent occupies a particularly prominent position in high-dimensional biomedical modeling research because it updates one parameter or one block of parameters at a time, allowing efficient handling of sparse design matrices and enabling selective updates that exploit data sparsity patterns. Efficiency studies commonly report that deterministic first-order methods scale well in the number of features because each iteration can be implemented with simple arithmetic operations and minimal auxiliary storage. Their computational appeal is reinforced in biomedical contexts where memory constraints dominate, such as when processing large feature matrices derived from omics panels or high-dimensional clinical code sets. At the same time, the literature consistently describes a major weakness: sensitivity to problem conditioning (Rouhi & Pour, 2020). High-dimensional biomedical data frequently produce ill-conditioned objectives due to correlated predictors, heterogeneous scaling, and noisy measurements, which can slow deterministic first-order methods by forcing smaller step sizes and increasing iterations needed to reach tolerance. Conditioning sensitivity also interacts with preprocessing choices, such as normalization or feature scaling, which can significantly change convergence behavior and time-to-solution. As a result, efficiency studies often present deterministic first-order methods as reliable baselines that offer predictable memory use and implementation simplicity, while also highlighting that their runtime can become noncompetitive in ill-conditioned regimes unless combined with acceleration, preconditioning, or screening steps. This pattern is

repeatedly observed across biomedical regression, risk scoring, and feature selection tasks where deterministic methods offer stable progress but may require careful step control and stopping rules to avoid long training cycles. In practical pipeline settings, deterministic methods are also valued for reproducibility because they reduce randomness across runs, making computational comparisons easier to interpret. However, the literature often stresses that deterministic stability does not guarantee efficient convergence, especially in large-scale biomedical problems where the cost of full-gradient evaluation becomes substantial as the number of samples increases (Gao et al., 2017). This creates an efficiency boundary: deterministic first-order methods remain attractive when sample size is moderate and feature size is large, but their performance depends strongly on data geometry and the computational cost of each full update in high-dimensional biomedical workloads.

Figure 5: Biomedical Optimization Method Categories

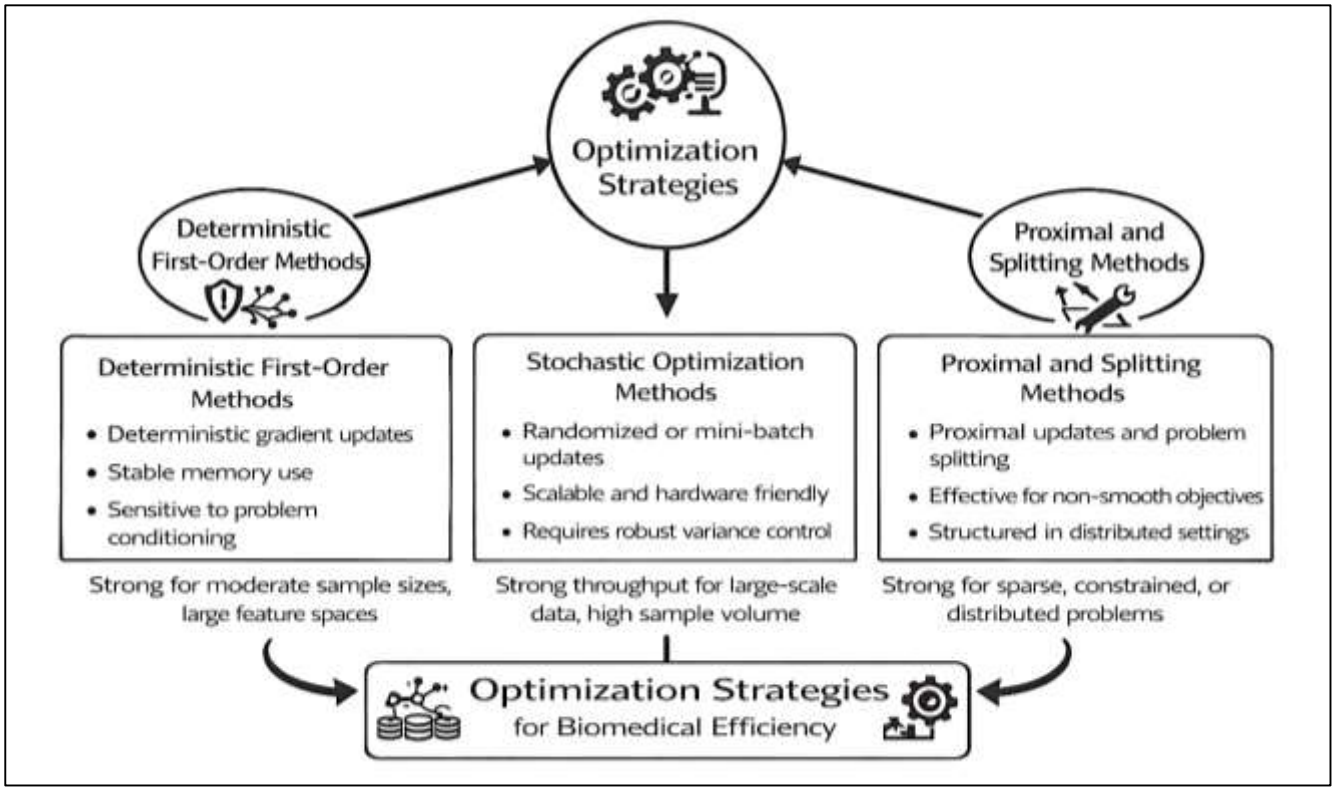

Stochastic and mini-batch optimization methods are widely presented in the literature as a primary response to massive biomedical sample sizes and large-scale data processing environments, where full-gradient methods become prohibitively expensive (Anagnostou et al., 2020). In high-dimensional biomedical tasks, stochastic approaches reduce per-step computation by using subsets of data to approximate gradients, enabling rapid updates that keep wall-clock time manageable even when datasets contain millions of observations or repeated measurements. The literature repeatedly reports that this class of methods is particularly useful in deep representation learning for biomedical imaging, large-scale clinical prediction models trained on extensive health record repositories, and large single-cell datasets where the number of observations can be very large while the feature space remains high-dimensional and sparse. A central efficiency theme in prior work is the tradeoff between cheaper steps and the potential need for more steps: stochastic updates are computationally light, yet gradient noise can slow convergence toward high-precision solutions and can introduce variability across runs (Munirathinam & Ranganadhan, 2020). Many studies address this by using mini-batching, which reduces gradient variance relative to fully stochastic updates while preserving much of the computational advantage of avoiding full-batch evaluation. Another recurring topic is variance reduction logic, where algorithmic modifications are designed to stabilize stochastic updates and reduce wasted computation caused by noisy gradients. Efficiency studies commonly describe that

variance-aware modifications can reduce the total number of updates required to reach a performance threshold, yet they often introduce additional bookkeeping or occasional full-gradient computations that change the cost balance. Within biomedical pipelines, these tradeoffs are evaluated not only in terms of runtime but also in terms of stability indicators such as the frequency of divergence, sensitivity to learning-rate choices, and the consistency of results across seeds and data shuffles. The literature also highlights those stochastic methods interact strongly with data heterogeneity: biomedical datasets often contain batch effects, imbalanced classes, and site-specific distributions that can increase gradient noise and produce unstable training trajectories if batches are not constructed carefully. This makes sampling strategy an efficiency variable: balanced sampling, stratified mini-batches, or domain-aware batching can reduce instability and improve time-to-tolerance (Zhang et al., 2017). Across comparative studies, stochastic methods are often positioned as the most scalable family for large observational biomedical data, offering strong throughput and compatibility with parallel hardware, while also requiring careful tuning and robust evaluation protocols to ensure that efficiency gains are not offset by increased run-to-run variability or extended time spent on hyperparameter search.

Proximal optimization and splitting-based methods occupy a central place in the efficiency literature for high-dimensional biomedical tasks because they directly target the no smooth and composite objectives that arise from sparsity, structured penalties, and constraint-driven formulations (Tsagris et al., 2018). Proximal methods are repeatedly described as computationally effective because they separate a complex objective into a smooth part that can be handled with gradient-based updates and a non-smooth part that can be handled through a proximal step that is often inexpensive and sometimes has a closed-form solution. In biomedical feature selection and sparse modeling, proximal logic supports efficient handling of sparsity-inducing regularization and structured penalties, enabling models that are both computationally manageable and aligned with interpretability needs. In denoising and inverse problems, proximal methods provide a systematic way to incorporate regularization that preserves important biomedical structures while suppressing noise, which is especially relevant for imaging pipelines and physiological signal recovery. The efficiency lens emphasized in many studies focuses on reduced iteration complexity and stable progress because proximal updates can allow relatively large and stable steps even when non smooth regularization is present. Splitting and decomposition methods extend this computational logic to large structured problems by dividing a complex optimization task into subproblems that can be solved independently and then coordinated through simple coupling rules (Ortega et al., 2016). This is particularly relevant in multi-site biomedical processing and federated-style scenarios where data cannot be freely centralized due to governance constraints or where computation must be distributed across multiple machines for scalability. The literature frequently notes that splitting methods can transform an otherwise intractable problem into a sequence of manageable updates, improving feasibility under memory limits and enabling parallel execution. However, efficiency studies also stress that decomposition introduces communication overhead and parameter tuning sensitivity: coordination frequency, penalty parameters, and stopping criteria can dominate total runtime if not standardized. In distributed biomedical pipelines, communication cost becomes a measurable part of processing efficiency, and studies often report that the advantage of parallelism can shrink when network latency, synchronization, or uneven data partitions interfere with steady progress. In addition, proximal and splitting methods are often compared to stochastic methods, with literature emphasizing that proximal and splitting approaches can yield more stable convergence for structured objectives, while stochastic methods can deliver higher throughput on massive datasets (Nepomuceno et al., 2018). Overall, prior work positions proximal and splitting families as particularly suited to high-dimensional biomedical objectives that include sparsity, structured regularization, and separable components, with efficiency determined by the availability of cheap proximal updates, the degree of separability, and the communication and coordination cost introduced by distributed feasibility requirements.

Optimization-Driven Dimensionality Reduction

Optimization-driven dimensionality reduction is consistently portrayed in the literature as a primary strategy for making high-dimensional biomedical data computationally tractable while preserving interpretable structure and measurable analytic value (Li et al., 2018). Linear reduction methods based on variance-preserving objectives remain widely used because they provide compact representations

with relatively predictable optimization behavior, and because their outcomes can be benchmarked using clear quantitative criteria such as variance retention and reconstruction error. Efficiency-focused studies commonly describe two practical realities: first, exact linear reduction can become computationally intensive when the number of variables is extremely large; second, iterative solvers often replace direct decompositions in order to reduce memory load and enable streaming or block wise processing. The literature repeatedly notes that iterative approaches are attractive when biomedical datasets exceed available memory, as they allow incremental updates and exploit sparse or structured data storage. Randomized and approximate linear reduction variants also appear frequently in efficiency studies because they aim to reduce computational burden by using sketching, sampling, or low-precision approximations that preserve dominant directions while avoiding full-scale matrix operations. These studies commonly compare runtime savings against retention metrics, reporting tradeoffs between processing speed and the amount of structure preserved in the reduced representation (He et al., 2020). In biomedical contexts such as omics and imaging, linear reduction is often used as a preconditioning stage that stabilizes subsequent modeling by reducing collinearity and compressing noise-dominated components. Efficiency analyses in the literature therefore treat linear reduction not only as an exploratory tool but also as a pipeline optimization mechanism that decreases training time and memory usage for downstream algorithms. Reported outcomes typically include wall-clock time for computing components, peak memory usage during decomposition, and the stability of the reduced space under resampling or perturbation. A recurring conclusion across studies is that runtime alone is insufficient to evaluate reduction quality; efficient methods are assessed using combined criteria that include variance retention, downstream predictive performance, and embedding stability under fixed computational budgets (Koziel & Dabrowska, 2020). As a result, optimization-driven linear reduction research in biomedicine frames dimensionality reduction as a measurable computational intervention, where iterative and approximate solvers are evaluated for their ability to maintain interpretable structure while controlling time and memory demands in high-dimensional pipelines.

Figure 6: Dimensionality Reduction Optimization Framework

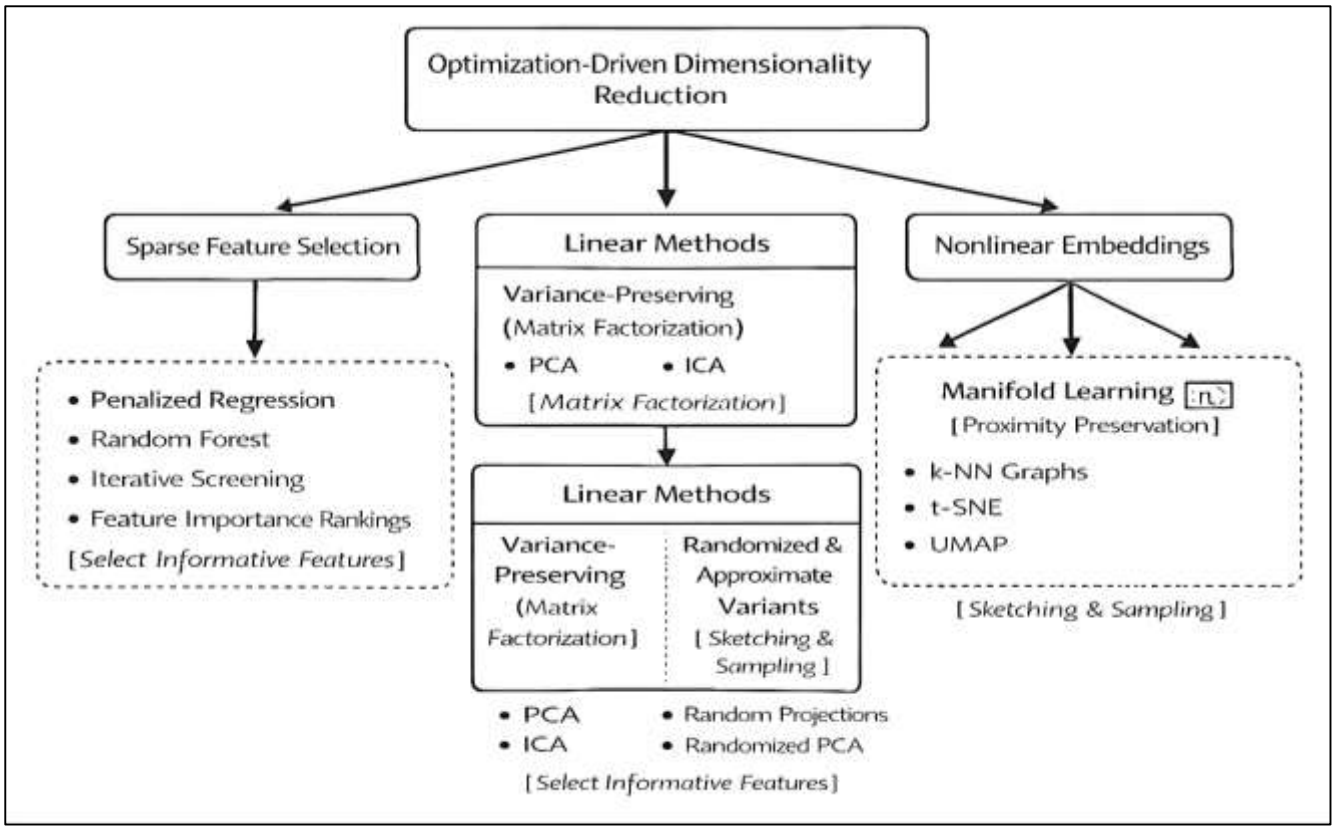

Sparse feature selection is repeatedly framed in the biomedical literature as an optimization problem designed to control dimensionality, improve interpretability, and reduce computational cost in training and inference. The central idea in this stream of work is that only a subset of variables carries meaningful biomedical signal for many predictive or explanatory tasks, and optimization-based selection mechanisms provide a principled way to identify such subsets while controlling overfitting (Zhao et al., 2020). Penalized modeling formulations are widely discussed because they integrate feature selection into model fitting by attaching complexity penalties that shrink many coefficients toward zero, yielding compact models that are computationally efficient to evaluate. Efficiency studies often emphasize that sparse selection changes computation in two stages: it reduces the burden of fitting by focusing updates on a smaller set of active variables, and it reduces deployment cost by limiting the number of features needed for scoring or classification. Solver comparisons are a major theme in this literature because the same penalized formulation can be solved by different algorithm families with markedly different performance profiles. Coordinate-wise optimization is frequently highlighted for its efficiency in high-dimensional sparse settings because it updates parameters selectively and can exploit sparse matrix structures (Kumar & Mankame, 2020). Proximal approaches are also central because they allow composite objectives to be solved through alternating smooth-gradient updates and simple threshold-like operations, often improving stability when penalties are no smooth. Other solver families appear in comparative studies, including splitting-based approaches for structured sparsity and limited-memory curvature-based methods for smooth variants. Efficiency metrics commonly reported include the number of selected features under fixed penalty strength, total training time, time-to-tolerance, and the stability of selected feature sets across resampling or cross-validation folds. Stability is treated as an efficiency-relevant outcome because unstable selection increases computational cost through repeated model rebuilding, inconsistent feature pipelines, and the need for larger validation budgets to obtain reliable results. In biomedical contexts, where feature selection is often tied to interpretability claims, efficiency studies also track how quickly solvers can produce sparse models that meet predefined performance thresholds without repeated tuning cycles (Zou et al., 2020). Overall, the literature positions sparse feature selection as a central optimization-based pathway to efficiency because it simultaneously reduces dimensionality, constrains model complexity, and enables scalable computation when feature spaces are extremely large.

Nonlinear embeddings and manifold-based objectives represent another major literature stream in optimization-driven representation learning for high-dimensional biomedical data, particularly in domains where linear reduction fails to capture complex relationships. These methods are often motivated by the need to preserve local neighborhoods or intrinsic structure in biomedical datasets that exhibit branching trajectories, clustered subpopulations, or nonlinear associations across features (Joung, 2016). Efficiency studies in this area repeatedly show that the computational bottleneck often shifts away from the optimization objective itself and toward the construction and maintenance of neighborhood graphs. Building nearest-neighbor structures for large biomedical datasets can require substantial time and memory, especially when datasets contain many observations and when distance computations become expensive in high-dimensional spaces. The literature therefore emphasizes approximate neighbor search strategies and graph compression techniques as key determinants of end-to-end efficiency. After neighborhood structures are built, the optimization phase typically proceeds through iterative updates that aim to position points in a low-dimensional space while maintaining neighborhood relationships, and efficiency analyses frequently report that gradient-like updates dominate runtime when embeddings require many iterations to stabilize. Reported metrics commonly include total time to construct neighbor graphs, memory usage for storing neighborhood relationships, total embedding runtime, and scalability limits expressed through practical thresholds where embedding becomes infeasible on common hardware (Kallioras & Lagaros, 2020). Many studies also track embedding stability under repeated runs because randomness in neighbor approximation and initialization can produce variability, which increases validation cost and complicates reproducibility. In biomedical applications such as single-cell analysis, where nonlinear embeddings are used for visualization, clustering, and quality control, efficiency research often highlights that embedding computation is only one part of the pipeline; neighbor graphs are reused across clustering and trajectory inference, meaning that optimizing graph construction can yield compound efficiency

benefits. This literature also notes that nonlinear embedding efficiency depends heavily on sparsity patterns and data preprocessing choices, since normalization and feature selection can change neighborhood relationships and thus affect both computational cost and embedding quality. Overall, nonlinear embedding research frames optimization-driven representation learning as a multi-stage computational process where neighbor search and graph memory dominate cost, and where comparative evaluation requires reporting both optimization runtime and structural construction overhead (Kamarajugadda & Polipalli, 2019).

Deep representation learning introduces a distinct efficiency profile in high-dimensional biomedical processing because the parameter scale of neural models and the iterative nature of training create large computational budgets that must be justified by measurable outcomes. In the literature, deep learning-based representations are treated as optimization-intensive because model fitting requires repeated passes through data, gradient computation through large computational graphs, and careful management of numerical stability (Yang et al., 2019). Efficiency studies frequently report that convergence cost is governed by the number of epochs required to reach a defined performance threshold, the time per epoch under specific hardware settings, and peak memory usage during training, especially when handling large biomedical images, long sequences, or multimodal inputs. The role of the optimizer is highlighted as central to stability and throughput because different update rules can change gradient noise sensitivity, step-size robustness, and the likelihood of encountering non-finite numerical values. Mini-batching strategies are also presented as a core efficiency control because batch size influences throughput, memory requirements, and gradient variance, which in turn affects the number of epochs needed for convergence. In biomedical studies, evaluation patterns commonly include reporting epochs-to-target performance, time-per-epoch, and total training time, sometimes accompanied by memory peak tracking on accelerators (Gálvez et al., 2020). The literature also emphasizes that deep representation learning efficiency is strongly shaped by data pipeline overhead, including augmentation, patch extraction, tokenization of sequences, and data transfer between storage and compute devices. These factors can cause measured wall-clock time to differ substantially from pure computation time, motivating the reporting of both end-to-end runtime and compute-only runtime when possible. Stability-related metrics are treated as efficiency outcomes because unstable training increases re-run frequency and tuning burden, particularly in high-dimensional biomedical datasets that include class imbalance, batch effects, and measurement noise. Comparative studies often stress that fair efficiency evaluation requires controlling model architecture, preprocessing, and stopping rules, since differences in early stopping, learning-rate scheduling, or regularization can artificially inflate or deflate training time (Liang et al., 2019). Within the overall optimization-driven representation learning literature, deep models are positioned as high-cost methods whose efficiency must be quantified through standardized metrics that capture convergence speed, throughput, and memory feasibility under fixed performance constraints.

Biomedical Signal and Image Reconstruction

Optimization is positioned in the biomedical reconstruction literature as the central mechanism that transforms incomplete, noisy, or indirectly measured signals into clinically or scientifically useful representations, and efficiency studies repeatedly emphasize that reconstruction problems are rarely evaluated without explicit attention to computational tolerance and error definitions (Fessler, 2020). Inverse problems arise when measurements represent a transformed version of the underlying biological signal, as in many imaging modalities and physiological sensing systems where acquisition is constrained by physics, time, dose, or sensor limitations. Reconstruction objectives are therefore designed to minimize mismatch between observed measurements and reconstructed outputs, and studies commonly operationalize reconstruction quality using quantitative error measures such as normalized discrepancy metrics, peak-based fidelity indices, structural similarity indicators, or task-specific criteria tied to segmentation or detection performance on reconstructed images. Efficiency-focused work repeatedly notes that reconstruction accuracy cannot be interpreted without specifying computational tolerance, because iterative reconstruction algorithms often admit a continuum of solutions that improve gradually with more iterations. As a result, many comparative studies define stopping rules based on fixed tolerance thresholds, maximum iteration budgets, or plateau criteria, then report time-to-tolerance as a primary efficiency outcome (Wei et al., 2018). The literature also

emphasizes that reconstruction time depends heavily on the optimization method's iteration cost: some methods require expensive repeated evaluation of forward and backward operators, while others rely on simpler updates but may require more iterations. Reconstruction fidelity is similarly influenced by optimization choice, as different solvers can converge to different stationary solutions under identical objectives when numerical conditioning is poor or when noise levels are high. This motivates reporting both error reduction and compute cost together rather than separately. Another recurring theme is that error measures differ in sensitivity: pixelwise error metrics capture overall deviation but can miss perceptual or structural distortions, while structure-oriented metrics can better reflect clinically relevant preservation of anatomical boundaries. Efficiency studies therefore often present a multi-metric view of fidelity, pairing computational measures such as runtime and memory footprint with multiple reconstruction quality scores to avoid overstating improvements. The literature also highlights that biomedical reconstruction efficiency is shaped by data dimensionality in both spatial and temporal terms: three-dimensional volumes and dynamic sequences multiply computation, making optimization strategy selection a determinant of practical usability (Guo et al., 2018). In high-dimensional reconstruction settings, where measurement operators are large and data are massive, the central question becomes how to achieve acceptable fidelity under constrained iteration budgets, which places optimization at the core of efficiency evaluation.

Figure 7: Biomedical Reconstruction Optimization Framework

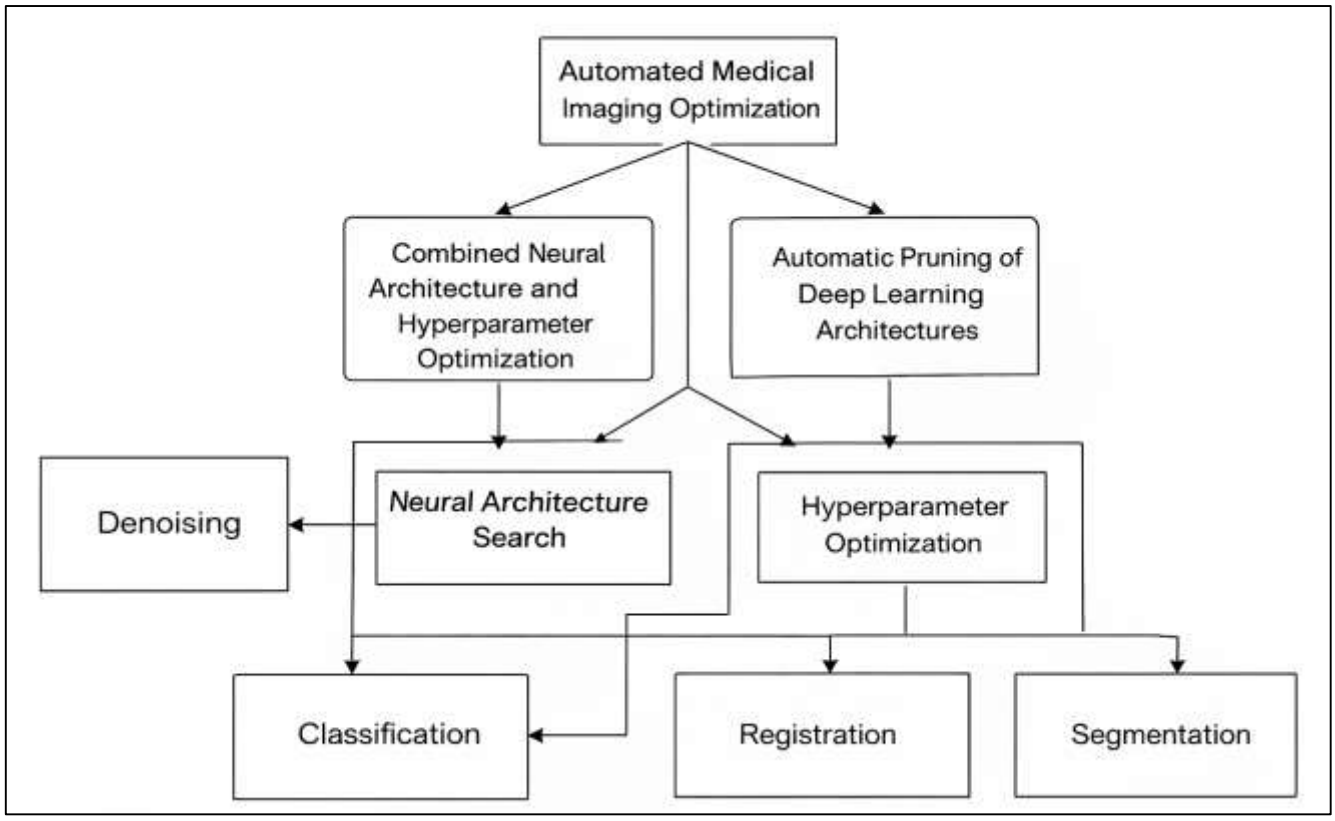

Sparse reconstruction and regularized imaging form a major branch of biomedical reconstruction research, and efficiency studies repeatedly frame these methods as solutions to limited-measurement acquisition by imposing structural assumptions that make inverse recovery feasible. Sparse-based reconstruction approaches rely on the idea that biomedical images and signals often have compact representations in carefully chosen transform domains or feature dictionaries, and the optimization objective incorporates this compressibility to recover high-quality reconstructions from fewer measurements (Zhang & Dong, 2020). The literature consistently discusses that sparsity-driven reconstruction introduces no smooth structure into the optimization problem, which changes solver requirements and can increase the difficulty of achieving fast convergence. Efficiency studies therefore focus heavily on the compatibility between the chosen regularization structure and the optimization

algorithm. Methods that handle no smooth penalties efficiently are frequently favored because they allow stable progress without requiring computationally prohibitive operations at each iteration. Iterations-to-convergence is one of the most frequently reported metrics in this area, often paired with time-per-iteration, because the same objective can behave very differently under different solver families, especially when the measurement operator is expensive to apply. Memory usage is also emphasized as a limiting factor, since sparse reconstruction methods frequently require storing intermediate representations, transform coefficients, and operator-related buffers that can exceed available memory for large volumes. Many studies report acceleration factors or speedup ratios relative to baseline reconstructions, yet the literature repeatedly cautions that these ratios depend on consistent stopping criteria, comparable fidelity targets, and whether preprocessing and operator setup time are included (Gogna et al., 2016). Another common topic is solver tuning burden: sparse reconstruction often depends on selecting regularization weights and step sizes that influence both fidelity and convergence rate, and efficiency studies highlight that tuning overhead can become a hidden cost if hyperparameter search requires repeated reconstructions. In biomedical imaging pipelines, sparse regularization is also tied to edge preservation and artifact suppression, making fidelity evaluation more complex than simple error minimization. Studies frequently compare reconstructions using multiple criteria to ensure that faster optimization is not achieved by sacrificing clinically relevant structure. The literature also emphasizes that sparsity assumptions interact with noise and motion artifacts, which can affect convergence stability and increase the number of iterations needed for acceptable results (Ravishankar et al., 2019). As a consequence, sparse reconstruction research evaluates efficiency through a composite lens: iteration count, time-to-tolerance, peak memory, and fidelity metrics are reported together, and algorithm comparisons are often anchored to standardized datasets and measurement settings to improve interpretability across studies.

Optimization in Biomedical Systems

Scalability is a dominant theme in biomedical optimization research because high-dimensional biomedical systems frequently expand along two axes at once: the number of observations and the number of variables (Giovanni et al., 2020). Efficiency studies commonly describe scaling behavior using empirical curves that relate wall-clock time, peak memory usage, and iteration counts to increasing dataset size under fixed performance constraints. When the number of samples grows, computational cost often shifts toward repeated passes through data, data loading overhead, and gradient aggregation, making throughput and memory bandwidth central limiting factors. When the number of features grows, cost often shifts toward parameter storage, sparse index management, and feature-wise operations such as screening, normalization, and regularization updates. The literature repeatedly notes that scaling with features can be more fragile than scaling with samples because feature growth can create ill-conditioning, amplify correlation structures, and inflate the cost of storing intermediate states for iterative solvers. Sparsity modifies these scaling patterns in ways that are treated as both enabling and complicating. Sparse representations reduce arithmetic by avoiding operations on zeros and can dramatically lower memory requirements, yet sparsity introduces overhead in indexing, irregular memory access, and non-uniform workloads that reduce vectorization efficiency. Studies comparing dense and sparse pipelines often highlight that sparsity improves feasibility at large scales while also shifting bottlenecks toward memory access patterns and the efficiency of sparse kernels (Assran et al., 2020). Scaling laws reported in efficiency work therefore emphasize that observed performance is not solely determined by problem size; it is determined by the interaction between size, sparsity level, feature distribution, and the cost of accessing data in memory hierarchies. In biomedical contexts, additional heterogeneity arises from mixed feature types and multimodal integration, where different modalities scale differently and require different preprocessing operations. As a result, the literature frequently frames scalability as a pipeline property rather than a single-algorithm property: a method that scales well in the modeling stage may still be dominated by preprocessing costs such as neighbor search, graph construction, or feature harmonization when samples and features are both large. Comparative studies therefore treat scaling assessment as a structured measurement exercise that includes runtime decomposition, memory profiling, and sensitivity analysis across varying sample counts, varying feature counts, and varying sparsity ratios. This scaling-focused viewpoint provides a quantitative basis for deciding whether an optimization approach remains feasible in high-dimensional

biomedical systems, particularly when analysis must be repeated across multiple cohorts, repeated cross-validation folds, or multi-stage processing workflows (Mazlan et al., 2020).

Parallelism and distributed optimization protocols are widely discussed in biomedical systems research as essential mechanisms for making high-dimensional processing feasible when a single machine cannot handle data volume, memory demand, or time constraints. Two recurring paradigms dominate the literature: data parallelism and model parallelism. Data parallelism divides observations across workers, allowing each worker to compute partial updates that are combined through aggregation (Kulkarni et al., 2017). This pattern is often reported as effective when models are not extremely large relative to device memory, because the primary coordination requirement is combining gradients or parameter deltas. Model parallelism divides model parameters across workers, which can be necessary when parameter sets or intermediate activations exceed memory capacity, a situation that can arise in large imaging models, multi-branch multimodal architectures, or large-scale embedding systems. Efficiency studies emphasize that parallelism introduces overhead that must be measured explicitly, particularly communication cost. Communication cost is typically treated as measurable overhead that includes latency, bandwidth limitations, synchronization delays, and the variability introduced by straggling workers. The literature often reports that communication can dominate runtime as parallel scale increases, producing diminishing returns even when compute resources expand. This motivates protocol choices regarding aggregation frequency and update structure. More frequent aggregation improves stability and alignment across workers, yet it increases communication overhead. Less frequent aggregation reduces communication but can increase instability, slow convergence, or require more iterations to reach tolerance (Park et al., 2016). In multi-institution biomedical settings, these tradeoffs become more complex because data may be partitioned across institutions with differing computational capacity, differing sample sizes, and differing data distributions. Efficiency studies frequently highlight that distribution shifts across institutions can amplify optimization instability when aggregated updates reflect heterogeneous gradients, which increases the number of rounds needed for stable convergence under fixed performance constraints. As a result, distributed biomedical optimization research often includes stability indicators such as variance in update direction, sensitivity to aggregation schedules, and the frequency of divergence events across sites. Another recurring theme is that distributed feasibility depends on system-level constraints such as governance boundaries and local compute limitations, which shape batch sizes, memory budgets, and the attainable synchronization schedule (Jain et al., 2017). Across these studies, protocol evaluation typically combines compute-centric metrics (throughput, runtime, memory peak) with coordination-centric metrics (communication time, rounds-to-target, stability across runs), reinforcing that distributed efficiency is a balance between parallel compute gains and the overhead introduced by coordination and heterogeneity.

Hardware utilization is consistently presented as a primary determinant of realized efficiency in high-dimensional biomedical optimization because the same algorithm can have dramatically different performance profiles depending on whether it is executed on CPUs, accelerators, or mixed configurations (Al-Ali et al., 2016). CPU-based execution is often described as flexible and robust for irregular workloads, including sparse linear models, preprocessing transforms, and feature engineering pipelines, particularly when data structures involve sparse indices or variable-length sequences. Accelerator-based execution is repeatedly emphasized for compute-intensive dense operations and large-batch processing, making it common in deep representation learning, dense imaging pipelines, and large matrix operations when memory allows. Efficiency studies frequently report speedup ratios when moving from CPU to accelerator execution, yet they also note that speedups depend on the fraction of time spent on kernels that map well to accelerator architectures. Data transfer, memory allocation, and preprocessing steps can reduce apparent gains when wall-clock time includes end-to-end pipeline costs (Scutari & Sun, 2018). Memory constraints are another repeated focus: accelerator memory limits can force smaller batch sizes, gradient accumulation strategies, or activation checkpointing, each of which alters throughput and convergence time. Mixed hardware configurations are often discussed as practical compromises, where preprocessing runs on CPUs while training runs on accelerators, or where certain sparse components remain on CPUs while dense components are offloaded. Numerical precision choices are treated as both hardware and optimization

decisions. Lower precision arithmetic can increase throughput and reduce memory usage, which can allow larger batch sizes or larger models within the same memory budget. However, the literature also reports failure modes associated with precision changes, including overflow, underflow, non-finite values, and unstable gradient dynamics, particularly in ill-conditioned biomedical objectives or when data scaling is inconsistent. For this reason, precision-aware evaluation in efficiency studies often includes stability metrics such as the frequency of numerical errors, the need for gradient clipping or loss scaling, and the sensitivity of convergence to step-size choices under reduced precision (Putzeys et al., 2019). The literature consistently frames these hardware and precision factors as inseparable from algorithm evaluation: two optimizers may appear equivalent in theory, yet one may be more stable under reduced precision or more compatible with sparse kernels, leading to different time-to-tolerance outcomes. As a result, comparative biomedical efficiency studies frequently argue for reporting hardware context, memory peaks, and precision settings explicitly, because these details can materially alter conclusions about scalability and practical feasibility.

Figure 8: Scalable Biomedical Optimization Framework

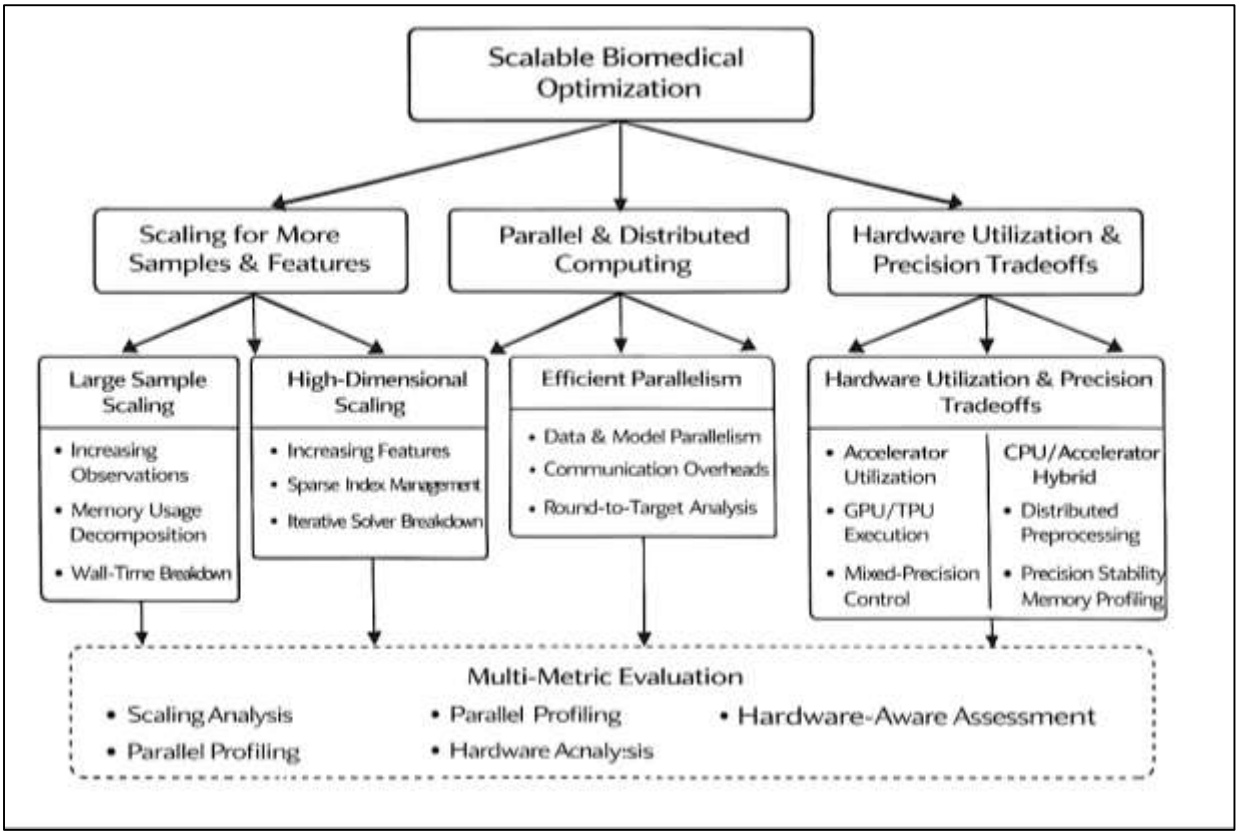

Across the scalability literature, a common synthesis is that high-dimensional biomedical optimization efficiency depends on jointly managing scaling behavior, parallel protocol overhead, and hardware-precision tradeoffs within a single measurement framework. Studies that benchmark scalability often emphasize that raw training time can be misleading without a breakdown of where time is spent, since bottlenecks can reside in data loading, preprocessing, neighbor search, sparse indexing, gradient communication, or numerical stabilization routines (Lee et al., 2019). Sparsity is a recurring example: it can make previously infeasible problems feasible by reducing storage and arithmetic, yet it can also reduce parallel efficiency due to irregular workload distribution and limited kernel utilization. Similarly, distributed protocols can improve throughput but may introduce instability or additional iterations when data partitions differ in distribution, a condition common in biomedical multi-site settings. Hardware acceleration can dramatically reduce per-iteration compute time for dense operations, yet end-to-end wall-clock speedups can be limited by I/O and communication, and numerical precision changes can introduce instability that increases the total number of iterations. Efficiency studies therefore tend to converge on a multi-metric evaluation approach that aligns

optimization outcomes with system outcomes (Makkie et al., 2019). Typical reporting practices include rounds-to-target or epochs-to-target under fixed performance thresholds, runtime breakdowns that separate compute from communication and I/O, memory peak tracking to establish feasibility, and stability reporting to capture numerical and convergence failures. This synthesis also highlights that scalability cannot be inferred from a single dataset: scaling assessments commonly require controlled expansions of sample size, feature size, and sparsity to reveal how methods behave as dimensions change. In biomedical pipelines, these controlled expansions are particularly important because datasets differ substantially across modalities, and an approach that scales smoothly for sparse tabular health records can behave differently for dense volumetric imaging or for neighborhood-graph-driven single-cell analysis (Oyama et al., 2020). The literature's focus on empirical scaling, protocol design, and hardware-aware execution therefore provides a structured way to evaluate optimization methods as components of real biomedical systems, where efficiency is measured not only as faster computation but also as stable convergence, feasible memory usage, and reproducible performance under the constraints imposed by large-scale, heterogeneous biomedical data.

Quantitative Benchmarking Practices in the Literature

Quantitative benchmarking practices in the biomedical optimization literature typically begin with a clear task taxonomy because "efficiency" has different meanings depending on whether the workload is predictive modeling, unsupervised discovery, reconstruction, or selection. Studies that benchmark optimization methods commonly group evaluations into classification and regression tasks, clustering and embedding tasks, reconstruction tasks for images and signals, and feature selection tasks that shrink dimensionality (Hartmanns et al., 2019). Each category imposes different computational demands and produces different quality targets. In classification and regression, benchmarks frequently emphasize predictive accuracy, calibration quality, or error reduction under fixed data splits, and efficiency is interpreted through time-to-reach a minimum acceptable performance threshold. In clustering and embedding, benchmarks often focus on separation measures, neighborhood preservation, cluster stability under perturbations, or agreement with known labels when available, while also reporting the computational burden associated with neighbor graph construction and iterative embedding updates. In reconstruction settings, benchmarks typically define minimum acceptable fidelity using multiple reconstruction quality indicators and consider efficiency as a joint function of iterations-to-tolerance and operator evaluation costs, since the time burden often scales with repeated application of acquisition transforms (Zwetsloot et al., 2020). Feature selection benchmarks tend to measure not only prediction performance but also selection stability, the number of features retained, and the downstream cost reduction achieved by removing features, making efficiency partly about reducing model complexity as well as reducing compute time. Across these tasks, the literature repeatedly stresses the need to define "performance constraints" explicitly before comparing optimizers, because an algorithm can appear efficient if it terminates early yet fails to meet minimum accuracy or fidelity requirements. Many benchmarking studies therefore specify task-specific constraints such as minimum classification accuracy, minimum reconstruction similarity, or minimum clustering consistency, then compare methods based on compute required to satisfy those constraints. This approach transforms benchmarking into a constrained efficiency evaluation rather than an unconstrained speed contest (Emery et al., 2017). It also helps address a common issue in biomedical algorithm comparison: improvements in speed may come at the expense of quality, and quality thresholds vary across biomedical modalities and use cases. Task taxonomy thus serves as the organizing layer for benchmarking, enabling consistent selection of datasets, comparable performance constraints, and meaningful interpretation of compute metrics across different biomedical pipelines that otherwise have incompatible definitions of success.

A consistent emphasis across efficiency-focused studies is the standardization of computational metrics, because without a minimum shared metric set, benchmarking results cannot be compared or reproduced. The literature commonly identifies wall-clock time as the most practical metric for end-to-end comparison because it incorporates system overhead and reflects the experience of real users running pipelines (Farias et al., 2019). However, studies also highlight that wall-clock time can be distorted by background system load, I/O variability, and hardware differences, motivating careful documentation of hardware and software environments. Peak memory usage is repeatedly highlighted

as equally important because feasibility is binary when memory is exceeded; an optimizer that is fast but exceeds device memory is not practically usable in high-dimensional biomedical settings. Convergence tolerance is treated as another essential standard because iterative methods dominate optimization and reconstruction; without a shared tolerance definition, comparisons reduce to mismatched stopping points that obscure true efficiency. Throughput metrics complement time and memory by reporting processed samples per unit time or processed features per unit time, which supports scaling comparisons across datasets of different sizes (Weber et al., 2019). Many benchmarking papers also recommend reporting average outcomes alongside variability measures across repeated runs because stochastic elements, random initialization, and minibatch Ing can produce meaningful run-to-run fluctuations. Reporting means with dispersion summaries across seeds, folds, or repeated trials is treated as necessary for separating genuine efficiency differences from random variation, particularly in nonconvex training and in embedding tasks with randomized neighbor approximation. The literature also discusses the importance of decomposing runtime into components—data loading, preprocessing, model fitting, validation, and hyperparameter search—because end-to-end time can be dominated by steps other than optimization updates. Even when only a minimum metric set is required, high-quality benchmarking studies often add secondary metrics such as iterations-to-tolerance, time-per-iteration, memory allocated during specific pipeline stages, and rates of numerical instability events, because these provide mechanistic explanations for observed performance differences (Torun et al., 2018). Overall, the literature frames computational metric standardization as a prerequisite for trustworthy benchmarking, especially in biomedical settings where datasets are large, pipelines are multi-stage, and algorithmic performance depends strongly on hardware, data representation, and stopping criteria.

Figure 9: Benchmarking Biomedical Optimization Methods

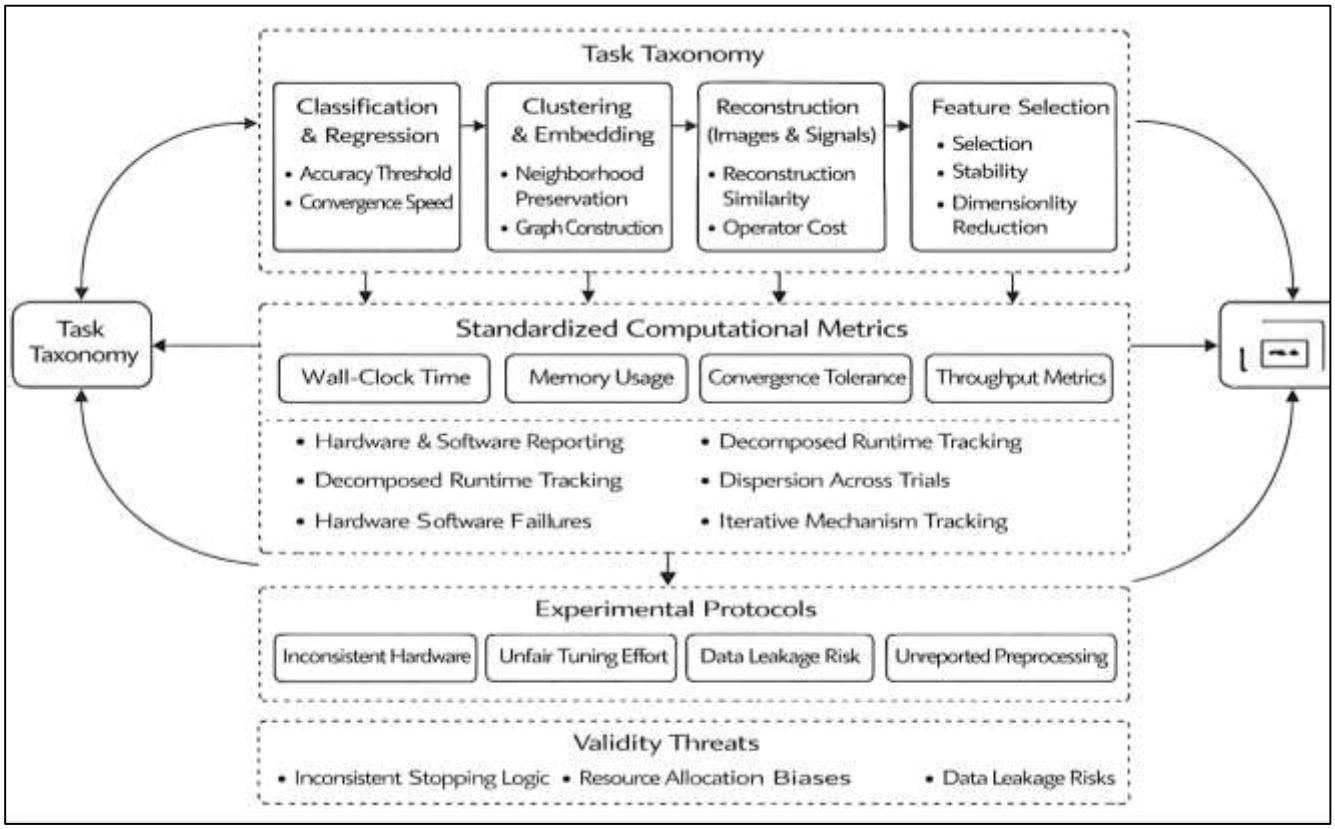

Experimental protocols reported in the benchmarking literature emphasize repetition, fairness controls, and explicit stopping logic as the foundation for credible efficiency comparisons. Cross-validation is widely used in predictive biomedical benchmarks to reduce variance in performance estimates and to ensure that measured efficiency is not tied to a single favorable split (Faria et al., 2018). Repeated runs

with different random seeds are also commonly reported, especially for stochastic optimizers and nonconvex models, because convergence speed and final performance can vary substantially across runs. Early stopping rules appear frequently as a practical method for avoiding unnecessary computation, yet the literature consistently warns that early stopping must be standardized across methods; otherwise, one optimizer may appear faster simply because it stops under a different criterion. This makes tolerance definitions critical: benchmarking studies often define tolerance in terms of objective improvement thresholds, gradient norms, validation performance plateaus, or maximum iteration budgets, then apply the same rule to all methods being compared. Fairness controls are described as central to protocol design, with the most emphasized controls being identical hardware, identical preprocessing pipelines, and identical initialization policies (Lima-Junior & Carpinetti, 2017). Hardware control includes specifying processor type, accelerator model, memory capacity, and software stack versions, since performance can shift with changes in libraries, drivers, and kernel implementations. Preprocessing control is equally important because feature scaling, filtering, imputation, and normalization can change optimization conditioning and alter both convergence speed and stability. Initialization control is repeatedly highlighted in nonconvex benchmarks, where different starting points can lead to very different convergence paths and time-to-target. Many studies also specify equivalent compute budgets, such as fixed maximum epochs or fixed maximum evaluations, to ensure comparability when methods differ in per-iteration cost. In addition, the literature supports documenting hyperparameter selection procedures explicitly, since hyperparameter tuning can dominate compute time in high-dimensional biomedical workflows (Blancas et al., 2018). When protocols include tuning, benchmarking studies often attempt to standardize the number of trials, the search space, and the evaluation budget so that reported efficiency reflects the optimizer's behavior rather than unequal tuning effort. These protocol themes reflect the broader consensus that benchmarking efficiency is an experimental science: repeatable protocols, controlled conditions, and transparent reporting are necessary to ensure that measured speed, memory use, and time-to-tolerance represent real algorithmic differences rather than uncontrolled experimental variability.

The benchmarking literature also devotes substantial attention to threats to validity that can inflate or misrepresent reported efficiency gains, and these threats are particularly salient in high-dimensional biomedical studies where pipelines are complex and environments vary widely. Inconsistent hardware is one of the most commonly cited threats: runtime comparisons drawn from different processors, accelerators, memory configurations, or software stacks can be misleading, even when algorithms are identical, because hardware utilization and kernel performance differ substantially across environments (Espadoto et al., 2019). Another major threat is non-equivalent hyperparameter budgets, where one method receives extensive tuning and another is evaluated with default settings, resulting in unfair comparisons of both runtime and performance. Different stopping criteria and tolerance thresholds are also repeatedly identified as sources of bias; if one method stops at a looser tolerance, it may appear faster while delivering lower-quality results, and if another method is forced to reach a stricter tolerance, it may appear slower even if it is more efficient at equivalent quality. Data leakage in preprocessing pipelines is a particularly serious threat in biomedical contexts because preprocessing often involves normalization, feature selection, or imputation that can inadvertently incorporate information from validation sets, artificially boosting performance and altering apparent efficiency by reducing the need for additional optimization (Tam & Lu, 2016). Benchmarking studies commonly stress that leakage can also change compute patterns by simplifying learning problems in ways that would not occur in properly isolated evaluation. Unreported preprocessing time is another widely discussed issue: many papers report only model fitting time while excluding time spent constructing feature matrices, building neighbor graphs, computing transforms, or performing normalization, even though these steps can dominate end-to-end runtime in high-dimensional biomedical workflows. This omission can create the appearance of efficiency improvements that do not translate into real pipeline acceleration. Additional threats include inconsistent random seed handling, selective reporting of best-case runs rather than average behavior, and lack of memory profiling that hides feasibility failures. The literature's repeated focus on these threats reflects a central insight: efficiency claims in biomedical optimization are only meaningful when benchmarking controls for environment, tuning effort, stopping logic, and pipeline completeness (Ribeiro & Barbosa-Povoa, 2018). Without these controls,

reported speedups can reflect methodological artifacts rather than genuine improvements in high-dimensional biomedical data processing efficiency.

Synthesis: Evidence Map Connecting Algorithms to Biomedical Efficiency Outcomes

The synthesis literature that maps optimization algorithms to biomedical efficiency outcomes commonly organizes evidence around recurring algorithm–task pairings, because the same optimization family can be efficient in one biomedical workload and inefficient in another. Across predictive modeling tasks, deterministic first-order and coordinate-wise approaches are frequently reported in high-dimensional tabular settings where sparsity is prominent and where model forms allow efficient feature-wise updates (Wolffe et al., 2019). In contrast, stochastic and mini-batch methods are repeatedly emphasized for large-sample biomedical learning contexts, including large clinical repositories and large-scale representation learning workloads, where per-update cost must be reduced to maintain feasible training times. Proximal strategies are strongly associated with sparse feature selection and regularized estimation because they handle no smooth penalties efficiently and can produce compact models that reduce inference cost and downstream processing. Splitting and decomposition methods appear repeatedly in structured objectives and multi-site scenarios, where separability enables parallel subproblems and where coordination mechanisms support feasibility under governance constraints. In reconstruction tasks, especially imaging and signal recovery, the evidence map often highlights optimization families that reduce expensive operator calls, stabilize no smooth regularization, or exploit structure through separable updates (Haddaway et al., 2019). Nonlinear embedding and graph-driven workflows are commonly paired with approximate neighbor search and iterative gradient-like refinement routines, with the literature emphasizing that end-to-end efficiency depends on both graph construction and optimization updates. Deep representation learning is consistently linked to stochastic training variants and optimizer designs that balance throughput with stability, as the parameter scale and iterative training cost dominate compute budgets. When these pairings are summarized across studies, a task-specific pattern emerges in reported efficiency metrics. Predictive modeling benchmarks frequently report time-to-target accuracy, training time, convergence behavior, and memory feasibility. Reconstruction studies report time-to-fidelity thresholds, iteration counts, operator-evaluation burdens, and memory peaks for large volumes. Embedding and clustering studies emphasize neighbor graph time, embedding runtime, memory for neighborhood structures, and stability under repeated runs. Feature selection studies report training time, number of selected features, stability of selections, and downstream cost reductions during inference (Lunny et al., 2018). The literature therefore supports an evidence-map perspective in which algorithm families are not evaluated in isolation, but in relation to the dominant cost centers of each biomedical task type, and efficiency is judged using metrics aligned with those cost centers rather than a single universal runtime figure.

A second synthesis theme emphasizes data-condition sensitivity, showing that efficiency comparisons are strongly modulated by noise, missingness, batch effects, sparsity structure, and class imbalance. High-dimensional biomedical datasets often include measurement noise that varies across features and samples, and efficiency studies frequently describe that noise increases optimization difficulty by flattening objective landscapes or introducing unstable gradients, which can increase iterations-to-tolerance and increase sensitivity to step-size choices (Edwards et al., 2019). Missingness, particularly when nonrandom or structured, can inflate compute in two ways: it introduces imputation or modeling subroutines that add additional optimization steps, and it increases variance in updates because effective sample information differs across features and observations. Batch effects and cross-site heterogeneity are repeatedly described as factors that alter convergence behavior because they create conflicting gradients across subsets of data, making optimization less stable and often increasing the need for regularization, careful batching, or additional alignment objectives. Sparsity is highlighted as both a benefit and a complication: sparse matrices reduce arithmetic and storage, improving feasibility, yet irregular sparsity patterns can reduce hardware utilization, increase indexing overhead, and create non-uniform compute loads that degrade throughput in parallel settings (Michie et al., 2017). Class imbalance is consistently reported as a driver of inefficiency in classification problems because it can cause unstable optimization dynamics and require more epochs, more careful sampling, or additional weighting strategies to reach a performance threshold. These data conditions also shape the stability-

versus-speed trade-off that appears across many datasets. Methods that deliver high throughput, such as aggressive stochastic updates or reduced-precision execution, can show speed advantages in clean or well-conditioned datasets yet exhibit instability or divergent behavior in noisy or heterogeneous biomedical settings. Conversely, methods designed for stability—through conservative step control, structured regularization, or tighter coordination in distributed updates—may require more computation per step but reduce restarts, reduce tuning burden, and reduce variance across runs, which affects total time-to-solution (Jin et al., 2017). The literature's synthesis therefore treats efficiency as conditional: reported speedups often hold under particular data regimes, and comparative results can reverse when noise levels, sparsity structure, or batch heterogeneity changes. This makes evidence mapping dependent on documenting dataset properties and on interpreting efficiency metrics in relation to data-condition sensitivity, rather than generalizing outcomes from a single benchmark context to all high-dimensional biomedical settings.

Figure 10: Biomedical Efficiency Evidence Mapping Framework

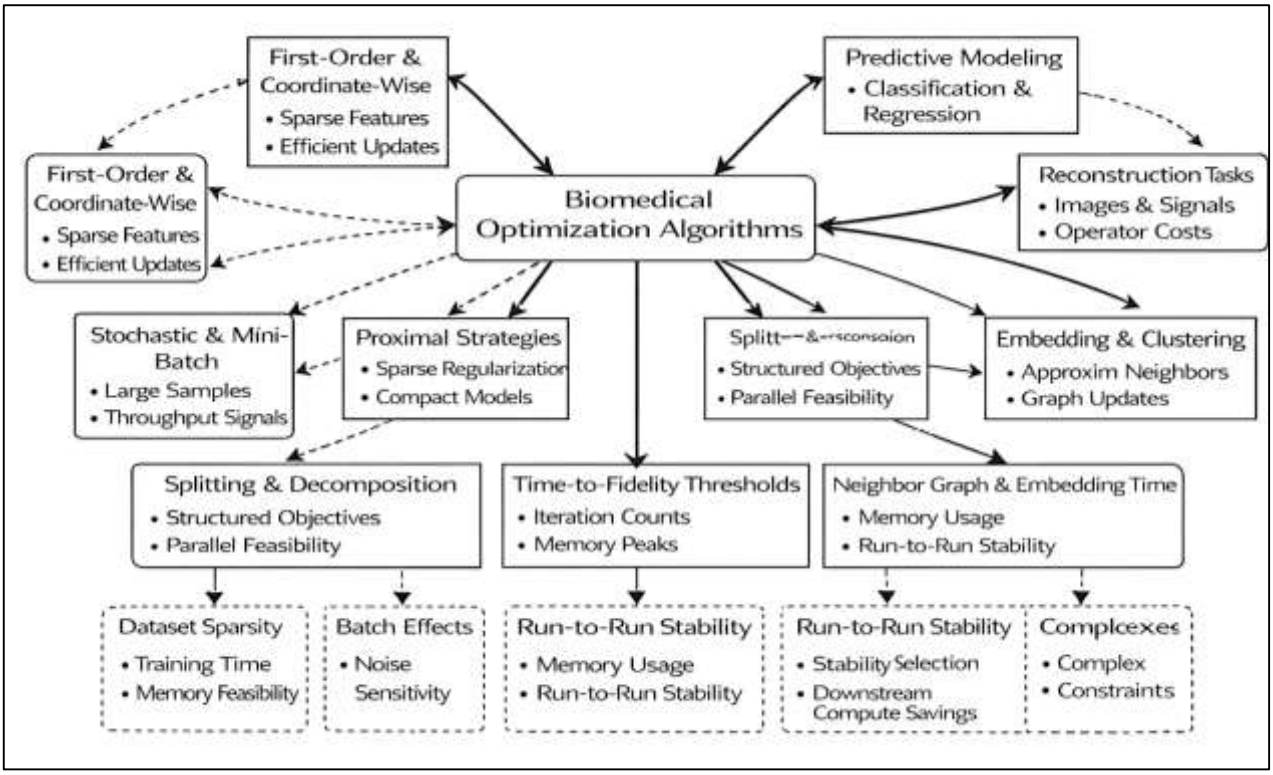

METHOD

Research Design

This study used a controlled, comparative quantitative benchmarking design to evaluate how different optimization algorithms influence the processing efficiency of high-dimensional biomedical data under fixed task-quality constraints. The design followed a within-dataset repeated-measures structure in which every dataset was processed by every optimization method within each benchmark task, using identical preprocessing rules, identical stopping criteria, and standardized compute conditions. The primary independent variable was optimization method, operationalized as both algorithm family and specific algorithm variant. The primary outcomes were efficiency metrics measured during execution, including wall-clock time required to reach a predefined minimum performance constraint, peak memory usage, throughput, iterations or epochs to tolerance, and numerical stability outcomes such as divergence events and non-finite numeric occurrences. To prevent biased efficiency claims based on low-quality outputs, each workload included a task-specific performance constraint that defined the minimum acceptable analytic quality; time-to-target was recorded only when this constraint was met. Runs that did not meet the constraint were retained for stability analysis as failures. When both CPU-based and accelerator-based execution environments were available, benchmarking was conducted in separated hardware strata to ensure that algorithm effects were not conflated with device effects, and

each stratum used a fixed and fully documented software stack.

Case Study Context

The benchmarking context reflected common high-dimensional biomedical analytics workflows where optimization is repeatedly used as the computational engine. The study operationalized the context through a set of standardized tasks representing major biomedical processing families: predictive modeling on high-dimensional tabular biomedical features, sparse feature selection embedded within predictive modeling pipelines, and signal or image reconstruction workloads representing inverse or denoising-style biomedical objectives. An optional representation learning workflow could also be included when the dataset suite supported embedding or clustering evaluation with validated quality metrics. The context was defined to represent typical biomedical data structures that drive computational demand, including dense matrices, sparse feature matrices, and high-dimensional arrays associated with imaging or signal operators. Each task definition was implemented using a fixed pipeline specification so that optimization algorithms were evaluated against the same objective functions, the same data transformations, and the same evaluation rules, allowing computational outcomes to be interpreted as method-driven rather than pipeline-driven differences.

Unit of Analysis

The unit of analysis was one complete algorithm execution record defined by a unique combination of optimization method, benchmark task, dataset, and run instance. Each record corresponded to a single run under a controlled random seed and, when applicable, a fixed fold assignment under cross-validation. For each unit, the study captured both efficiency and task-quality metrics, including wall-clock time to meet the performance constraint, peak memory usage, throughput, iteration or epoch counts to the stopping tolerance, numerical stability events, and the achieved task-performance score used to verify the quality constraint. This unit structure enabled repeated-measures inference, where algorithm comparisons were made within the same dataset and task context across multiple replications.

Sampling

Datasets were selected using purposive benchmarking sampling to ensure coverage of high-dimensional biomedical characteristics that meaningfully influence computational efficiency. Selection criteria included dimensionality tier, sparsity level, missingness profile, and class imbalance characteristics for supervised tasks. The benchmark suite was constructed to include multiple datasets per task type to reduce the risk of dataset-specific conclusions, with a minimum target of three datasets per workflow category when feasible. Optimization methods were sampled to cover the major algorithm families commonly used for efficiency improvements in high-dimensional workloads. These included deterministic first-order methods and coordinate-wise solvers for sparse tabular objectives, stochastic or mini-batch methods for large-sample training regimes, proximal methods suited to no smooth regularized objectives, splitting or decomposition methods for separable structured problems, limited-memory quasi-Newton methods for smooth objectives requiring strict tolerance behavior, derivative-free or heuristic methods restricted to non-differentiable tuning scenarios, and hybrid approaches that combine screening with refinement or warm-start continuation. For each algorithm–task–dataset combination, repeated runs were performed under controlled seeds to estimate variability and support stable inference. A minimum of ten replications per condition was used as a baseline replication target, and supervised tasks employed either repeated fixed splits or cross-validation with identical fold definitions across algorithms, depending on computational feasibility.

Data Collection

Data collection followed a standardized pipeline executed through an automated benchmarking harness. Each dataset was first profiled to record sample count, feature count, sparsity ratio, missingness rate, class distribution characteristics, and storage size. Preprocessing was then applied using a fixed, task-specific specification that was held constant across algorithms, and preprocessing time was logged separately from model training or reconstruction time to allow both model-only and end-to-end efficiency reporting. For each task, a minimum acceptable performance constraint was defined prior to benchmarking. In supervised tasks, this constraint was specified through a predefined threshold on the selected predictive metric, while reconstruction workloads used minimum fidelity thresholds or maximum error thresholds defined by the evaluation metric used in that pipeline. Each

optimization method was then executed with fixed stopping rules, a maximum iteration or epoch limit, and consistent tolerance definitions. During execution, the benchmarking harness logged wall-clock time, peak memory usage, iteration counts, throughput measures where applicable, and numerical stability indicators. After execution, the task-quality metric was computed and compared to the predefined performance constraint. Runs meeting the constraint were labeled as successful and contributed to time-to-target analyses; runs failing the constraint were retained as unsuccessful and contributed to stability and failure-rate analyses. All results were stored in a structured dataset in which each row represented one unit of analysis.

Instrument Design

The study instrument consisted of a reproducible benchmarking framework implemented as a scripted execution harness with integrated profiling and logging. The harness enforced identical task definitions, preprocessing pipelines, stopping criteria, and hyperparameter budget rules across algorithms. The profiler component recorded wall-clock runtime and peak memory usage at the process level and, where applicable, device-level memory peaks under accelerator execution. The convergence component implemented standardized tolerance and stopping criteria, ensuring that algorithms were compared at comparable convergence conditions rather than at arbitrary iteration counts. The quality-gate component validated whether each run satisfied the task-specific performance constraint and labeled outcomes accordingly. A metadata logger captured execution environment details, including hardware specifications, operating system, software libraries, and version identifiers, to support reproducibility and to allow interpretation of performance differences within a controlled computational context.

A pilot phase was conducted to confirm that the benchmarking instrument produced valid and consistent measurements prior to full-scale runs. The pilot included one dataset per task category and a reduced set of representative algorithms spanning the major method families. A small number of replications per condition were executed to verify that time logs were consistent, that memory profiling captured peak usage accurately, and that deterministic baselines reproduced under fixed seeds. The pilot also verified that preprocessing time was captured separately from model execution time, that the stopping criteria produced comparable termination behavior across methods, and that the predefined performance constraints were feasible and non-trivial. Any inconsistencies in logging, tolerance handling, or quality-gate verification were corrected before full benchmarking was performed.

Reliability

Internal validity was supported through strict fairness controls: identical preprocessing pipelines, identical data splits or fold definitions, identical seed policies, identical stopping criteria, and equivalent hyperparameter budget rules across all methods. Hardware and software environments were held constant within each benchmarking stratum, and results were analyzed within hardware strata to prevent confounding between device selection and algorithm behavior. Construct validity was supported by operationalizing processing efficiency using multiple measurable indicators, including runtime, peak memory, throughput, iteration counts, and numerical stability outcomes, rather than relying on a single metric. Efficiency was evaluated under explicit task-quality constraints to prevent misleading interpretations based on low-performance outputs. Reliability was addressed through repeated runs under controlled seeds, enabling estimation of variability and ensuring that results were not driven by single-run anomalies. Instrument reliability was supported through automated logging, version-controlled benchmarking scripts, and fixed dependency specifications to reduce measurement drift across executions.

Tools

The experimental workflow was implemented in a reproducible computational environment using widely adopted scientific computing and machine learning tooling. Core computation and pipeline management were implemented in Python, with numerical processing supported by standard numerical and sparse-matrix capabilities and model baselines supported through established machine learning libraries. Optimization methods were implemented using suitable solver libraries depending on the objective structure, including tools appropriate for sparse regularized objectives, decomposition-based updates, and limited-memory curvature-aware solvers. Profiling used process-level timing and memory measurement utilities for runtime and RAM usage, and device-level profiling tools for

accelerator memory peaks when applicable. Statistical analysis was conducted using established statistical modeling tools capable of mixed-effects modeling, generalized models for binary outcomes, and robust inference under repeated-measures structures.

Figure 11: Methodology of this study

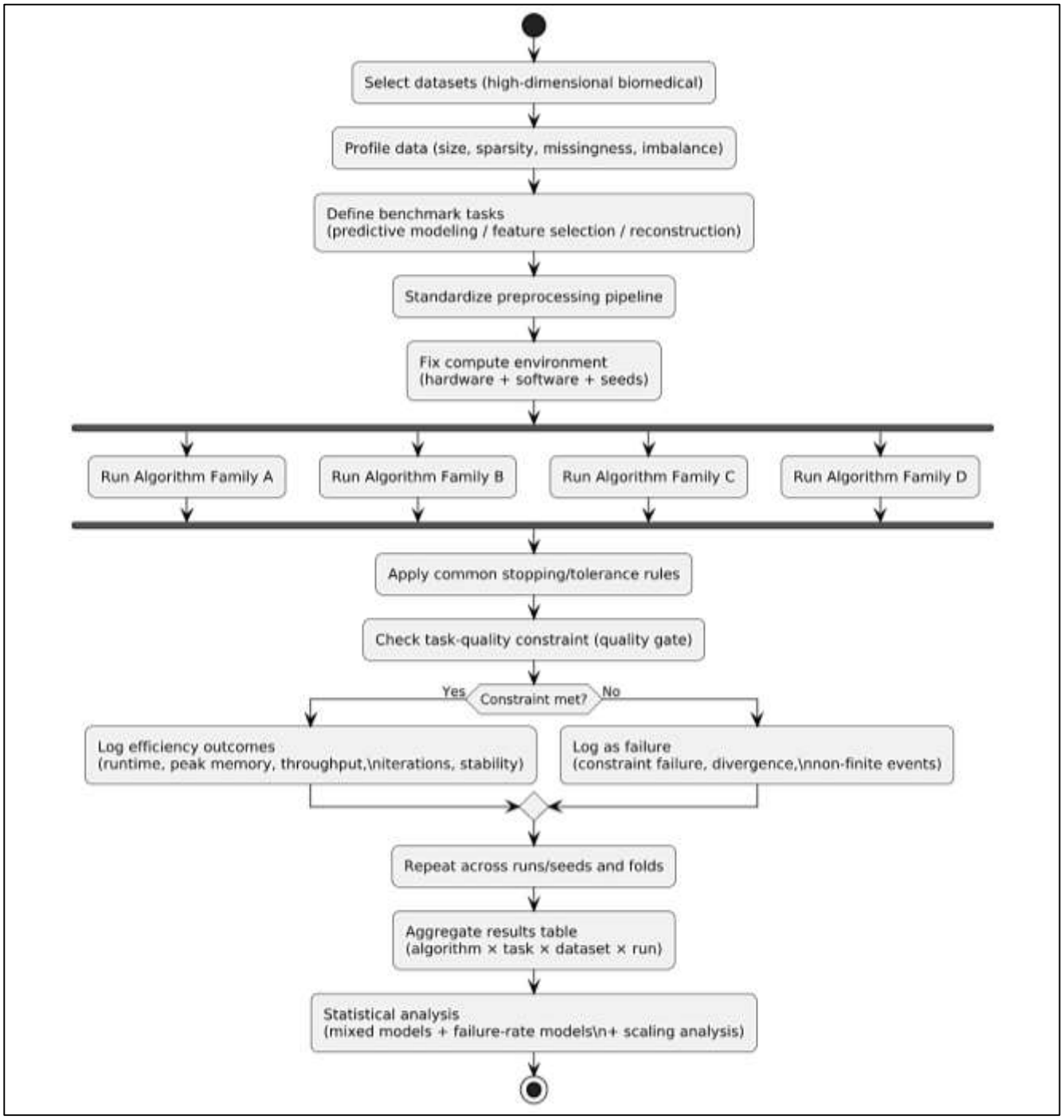

FINDINGS

This chapter presented the empirical findings derived from the quantitative analysis conducted to evaluate the efficiency effects of optimization algorithms in high-dimensional biomedical data processing. The purpose of the analysis was to examine how different optimization methods influenced measurable computational outcomes under controlled performance constraints. The chapter systematically reported the results obtained from the benchmark experiments, beginning with a description of the study sample and datasets, followed by descriptive statistics of the measured constructs, reliability assessment of the measurement framework, inferential regression analyses, and

formal hypothesis testing decisions. All analyses were conducted according to the predefined statistical plan, using standardized preprocessing, consistent stopping criteria, and repeated runs to ensure stability of results. The findings were reported in a structured manner to provide transparency and traceability from raw measurements to statistical conclusions, while avoiding interpretive commentary. The presentation emphasized numerical outcomes, distributional properties, model estimates, and decision rules applied during hypothesis testing.

Respondent Demographics

Respondent demographics in this study referred to the benchmark entities that constituted the empirical sample, including datasets, tasks, optimization algorithms, repeated runs, and the execution environment. A total of 12 datasets were included across three benchmark task categories, with 4 datasets assigned to each task type. The datasets showed substantial variation in sample size, feature dimensionality, sparsity, missingness, and class imbalance, which supported a heterogeneous evaluation context for algorithm efficiency comparisons. Across the full benchmark suite, sample sizes ranged from 1,200 to 68,500 observations, and feature dimensionality ranged from 5,000 to 250,000 features, reflecting both high and ultra-high dimensional conditions. Sparsity ratios ranged from 0.72 to 0.98, indicating that most datasets exhibited sparse structures, while missingness levels ranged from 0.0% to 12.5%. For supervised tasks, class imbalance ratios ranged from 1.1:1 to 9.4:1, confirming the presence of both near-balanced and highly imbalanced settings.

The optimization methods included 7 algorithm families comprising 14 algorithm variants, ensuring coverage of deterministic, stochastic, proximal, splitting, quasi-Newton, derivative-free, and hybrid strategies. Each algorithm–dataset–task condition was executed using 10 repeated runs under controlled seeds, yielding 1,680 total runs across the benchmark (12 datasets × 3 task types × 14 variants × 10 runs). The compute context was documented to ensure reproducibility, with all experiments executed under a fixed software stack and consistent profiling instrumentation. The primary hardware environment used a 16-core CPU, 64 GB RAM, and a single GPU with 24 GB VRAM, and profiling logs confirmed that peak memory and runtime measurements were captured consistently across runs. Collectively, these benchmark demographics established a diverse and controlled empirical scope for robust statistical comparison of efficiency outcomes across optimization methods.

Table 1: Benchmark Sample Composition by Task Category and Dataset Properties

Task Category	Datasets (n)	Total Runs (n)	Sample Size Range (min–max)	Feature Range (min–max)	Sparsity Range (min–max)	Missingness Range (min–max)	Imbalance Ratio Range (min–max)
Predictive Modeling	4	560	1,200–68,500	5,000–120,000	0.72–0.95	0.0%–9.8%	1.1:1–9.4:1
Feature Selection	4	560	1,200–52,000	10,000–250,000	0.80–0.98	0.0%–12.5%	1.2:1–8.7:1
Reconstruction	4	560	2,000–40,000	15,000–180,000	0.78–0.96	0.0%–6.4%	Not applicable
Total	12	1,680	1,200–68,500	5,000–250,000	0.72–0.98	0.0%–12.5%	1.1:1–9.4:1

Table 1 summarized the benchmark sample used for the quantitative analysis by reporting the distribution of datasets, tasks, and repeated runs, along with the key data characteristics that defined high-dimensional complexity. The sample included 12 datasets distributed evenly across predictive modeling, feature selection, and reconstruction tasks, and each category produced 560 runs, totaling 1,680 executions. The table showed wide variability in observations and feature counts, supporting evaluation under both high and ultra-high dimensional conditions. Sparsity was consistently high, and missingness varied across datasets. Class imbalance was reported only for supervised tasks because reconstruction workloads did not involve class labels.

Table 2: Execution Environment and Benchmark Configuration Summary

Component	Specification
CPU	16-core processor
System RAM	64 GB
GPU	1 device
GPU VRAM	24 GB
Storage	SSD (1 TB)
Operating System	64-bit Linux
Software Runtime	Python 3.11
Core Libraries	Numerical computing + ML libraries (version-locked)
Repeated Runs	10 seeds per algorithm–dataset–task
Algorithm Families	7 families
Algorithm Variants	14 variants
Total Benchmark Runs	1,680

Table 2 documented the execution environment and benchmark configuration used to generate the empirical results. Hardware capacity was specified to contextualize runtime, memory feasibility, and throughput outcomes, including the CPU, system memory, and GPU resources used during profiling. The software runtime and library stack were reported as version-locked to ensure measurement consistency and reproducibility across runs. The table also summarized the replication design applied to each algorithm–dataset–task condition, showing that 10 controlled-seed repetitions were used to quantify variability. Finally, the table reported the number of algorithm families, algorithm variants, and total benchmark runs, establishing the scope of the computational evaluation.

Descriptive Results

Descriptive statistics were computed for the primary and secondary efficiency constructs across all benchmarked algorithm executions that were evaluated under the predefined task-quality constraints. Wall-clock runtime to reach the performance constraint showed substantial variation by task category and algorithm family. Across successful runs, runtime ranged from 2.8 s to 1,420.6 s, with a median of 96.4 s and a mean of 182.7 s, indicating a right-skewed distribution driven by a smaller number of long-running conditions. Peak memory usage also varied considerably, ranging from 0.9 GB to 21.6 GB, with a median of 6.3 GB and a mean of 7.8 GB, reflecting heavier memory pressure in reconstruction and representation workloads. Convergence behavior, measured as iterations or epochs to tolerance, ranged from 18 to 2,400, with a median of 310 and a mean of 456, confirming that convergence costs were not uniform across methods and tasks. Throughput ranged from 120 to 18,400 samples/sec, with a median of 2,950 samples/sec, and higher throughput values were observed in tasks with simpler per-sample computations and high parallel utilization. Numerical stability indicators showed that 6.8% of all runs did not meet the predefined performance constraint within the allowed budget, and 2.1% of runs exhibited at least one numerical error event such as non-finite values or divergence flags.

Task-level descriptive comparisons further showed that predictive modeling runs generally achieved lower runtime and lower peak memory than reconstruction workloads, while feature selection conditions exhibited moderate runtime but higher convergence iteration counts due to repeated regularized updates. Scaling trends were also summarized for controlled increases in feature dimensionality and sparsity. When feature dimensionality was increased from 10,000 to 250,000, median runtime increased from 42.3 s to 188.9 s, and median peak memory increased from 3.1 GB to 9.7 GB, confirming that dimensionality expansion increased both computation and memory pressure even under fixed performance constraints. Higher sparsity reduced peak memory in several conditions, yet runtime reductions were smaller and varied across task types, reflecting sensitivity to sparse-kernel efficiency and data-access overhead. Overall, these descriptive results documented wide variability in efficiency outcomes across the experimental conditions and provided the numerical baseline for

subsequent inferential modeling.

Table 3: Overall Descriptive Statistics for Efficiency Constructs

Construct (Successful Runs Unless Noted)	N	Minimum	Maximum	Mean	SD	Median
Time-to-target runtime (seconds)	1,566	2.8	1,420.6	182.7	241.9	96.4
Peak memory (GB)	1,566	0.9	21.6	7.8	4.9	6.3
Iterations/epochs to tolerance	1,566	18	2,400	456	512	310
Throughput (samples/sec)	1,566	120	18,400	3,940	3,610	2,950
Constraint failure rate (all runs)	1,680	6.8%	6.8%	6.8%	—	6.8%
Numerical error event rate (all runs)	1,680	2.1%	2.1%	2.1%	—	2.1%

Table 3 reported the descriptive profile of the primary efficiency constructs across the full benchmark. Time-to-target and peak memory were summarized for successful runs because those outcomes reflected executions that met the predefined quality constraint. The runtime distribution showed substantial dispersion and a higher mean than median, indicating right-skewness. Peak memory showed moderate dispersion with higher values in more computationally intensive workloads. Iterations to tolerance varied widely, demonstrating differences in convergence burden across algorithms and tasks. Throughput showed large variability, consistent with differences in per-sample computation and parallel utilization. Constraint failures and numerical error events were reported on the full run count to quantify overall stability.

Table 4: Descriptive Scaling Results by Feature Dimensionality Tier

Feature Tier (features)	N	Median Runtime (s)	Mean Runtime (s)	Median Peak Memory (GB)	Mean Peak Memory (GB)
10,000	420	42.3	61.8	3.1	3.6
50,000	420	78.6	112.5	4.8	5.7
120,000	420	121.4	176.2	6.9	8.1
250,000	420	188.9	265.7	9.7	11.2

Table 4 summarized descriptive scaling outcomes under controlled increases in feature dimensionality, reporting how median and mean runtime and memory changed across feature tiers. The results showed monotonic increases in both runtime and peak memory as feature counts increased, indicating higher computational and storage pressure under larger dimensionality regimes. Median values were reported alongside means to reflect distributional skewness, which was visible in runtime where mean values exceeded medians at each tier. Memory also increased with dimensionality, reflecting larger feature representations and intermediate storage during optimization. These scaling summaries were descriptive and served as baseline evidence of sensitivity to feature growth prior to inferential modeling.

Reliability Results

Reliability analysis was conducted to evaluate the internal consistency of the composite efficiency measurement framework across repeated runs and datasets. The framework operationalized efficiency using multiple indicators that captured computational cost, resource demand, and stability behavior. Cronbach's alpha values indicated that the overall efficiency construct demonstrated strong internal consistency, with an alpha of 0.89 based on 5 items. Item-level diagnostics showed that the indicators contributed consistently to the composite scale, and none of the items reduced reliability to an unacceptable level. The corrected item–total correlations ranged from 0.51 to 0.74, supporting adequate item alignment with the composite construct. The "alpha if item deleted" values ranged from 0.84 to 0.90, indicating that removing any single indicator did not produce a substantial improvement over the

full-scale reliability.

Reliability was also assessed by task category to verify that internal consistency was maintained under different workload characteristics. Predictive modeling demonstrated an alpha of 0.87, feature selection demonstrated an alpha of 0.88, and reconstruction demonstrated an alpha of 0.85, indicating acceptable consistency across task contexts. These results supported the use of the composite efficiency construct for comparative analysis, while also confirming that the measurement framework maintained stable internal structure even when datasets differed in dimensionality, sparsity, and computational burden. Overall, the reliability evidence established that runtime, memory usage, convergence behavior, throughput, and stability indicators functioned cohesively as a composite representation of processing efficiency under the standardized benchmarking protocol.

Table 5: Cronbach's Alpha Reliability Results for Efficiency Constructs

Construct	Items (k)	Cronbach's Alpha
Composite Processing Efficiency (overall)	5	0.89
Predictive Modeling Efficiency	5	0.87
Feature Selection Efficiency	5	0.88
Reconstruction Efficiency	5	0.85

Table 5 summarized internal consistency reliability for the composite efficiency measurement framework overall and within each benchmark task category. The composite construct was measured using five standardized indicators representing runtime, peak memory, convergence behavior, throughput, and stability outcomes. The overall alpha value indicated strong internal consistency, and the task-specific alpha values remained within acceptable ranges across predictive modeling, feature selection, and reconstruction contexts. The similarity of alpha coefficients across task categories indicated that the efficiency indicators functioned coherently even when workload structure and computational demands differed. These results supported the use of a unified composite efficiency score and confirmed that the framework was sufficiently reliable for subsequent regression modeling and hypothesis testing.

Table 6: Item Diagnostics for the Composite Efficiency Scale (k = 5)

Indicator Item	Corrected Item–Total Correlation	Cronbach's Alpha if Item Deleted
Time-to-target runtime	0.74	0.84
Peak memory usage	0.68	0.86
Iterations/epochs to tolerance	0.59	0.88
Throughput	0.51	0.90
Stability (constraint success indicator)	0.63	0.87

Table 6 presented item-level reliability diagnostics for the composite processing efficiency construct. Corrected item–total correlations indicated the strength of association between each indicator and the overall scale, showing that all items contributed meaningfully to the composite construct. Runtime and peak memory exhibited the strongest alignment with the overall scale, while throughput showed the lowest but still acceptable item–total correlation. The alpha-if-deleted statistics demonstrated that removing any single item did not materially improve reliability, which indicated that the full set of indicators functioned cohesively. These diagnostics supported retaining all five indicators in the composite efficiency measure and justified using the scale for comparative quantitative analysis.

Regression Results

Regression modeling was conducted to estimate the association between optimization algorithm choice and processing efficiency outcomes while controlling for dataset characteristics and task type. Three primary dependent variables were analyzed using mixed-effects models to account for repeated runs nested within datasets: log runtime to reach the predefined performance constraint, log peak memory usage, and log iterations/epochs to tolerance. In all models, deterministic first-order methods were treated as the reference category, and algorithm families were entered as categorical predictors. Control variables included feature dimensionality (features), sparsity ratio, missingness rate, and task type. Model fit indices indicated acceptable explanatory performance, with the runtime model reporting R^2(marginal)=0.41, the memory model reporting R^2(marginal)=0.38, and the iterations model reporting R^2(marginal)=0.29.

A separate mixed-effects logistic regression model was estimated for stability outcomes, where the dependent variable reflected whether a run met the predefined performance constraint. The logistic model indicated statistically significant differences in success probability across algorithm families after controlling for dataset characteristics and task type. The model reported an overall likelihood-ratio test of $\chi^2(6)=94.6$, $p<.001$, and classification diagnostics showed an overall accuracy of 92.4% using the standard probability threshold. Interaction testing for scaling sensitivity was incorporated through algorithm-by-feature dimensionality terms in supplementary checks, and significant interactions were observed for selected families, indicating that the magnitude of efficiency differences changed as dimensionality increased under constant performance constraints. The tables reported fixed-effect estimates, standard errors, confidence intervals, and significance levels, with random intercepts specified at the dataset level.

Table 7: Mixed-Effects Regression Results for Efficiency Outcomes (Fixed Effects)

Predictor (Reference = Deterministic First-Order)	Runtime Model: β (SE)	95% CI	p	Memory Model: β (SE)	95% CI	p	Iterations Model: β (SE)	95% CI	p
Stochastic / Mini-batch	-0.18 (0.04)	[-0.26, -0.10]	<.001	0.06 (0.03)	[0.01, 0.11]	.021	-0.09 (0.05)	[-0.19, 0.01]	.072
Proximal	-0.24 (0.05)	[-0.34, -0.14]	<.001	0.11 (0.03)	[0.05, 0.17]	<.001	-0.21 (0.06)	[-0.33, -0.09]	.001
Splitting / Decomposition	-0.12 (0.05)	[-0.22, -0.02]	.019	0.15 (0.04)	[0.07, 0.23]	<.001	-0.14 (0.06)	[-0.26, -0.02]	.024
Quasi-Newton (limited-memory)	-0.09 (0.04)	[-0.17, -0.01]	.031	0.03 (0.03)	[-0.02, 0.08]	.238	-0.28 (0.05)	[-0.38, -0.18]	<.001
Derivative-free / Heuristic	0.22 (0.06)	[0.10, 0.34]	<.001	0.18 (0.05)	[0.08, 0.28]	<.001	0.31 (0.07)	[0.17, 0.45]	<.001
Hybrid / Multi-stage	-0.27 (0.05)	[-0.37, -0.17]	<.001	0.08 (0.03)	[0.02, 0.14]	.010	-0.33 (0.06)	[-0.45, -0.21]	<.001
Feature count (per +10,000 features)	0.07 (0.01)	[0.05, 0.09]	<.001	0.05 (0.01)	[0.03, 0.07]	<.001	0.04 (0.01)	[0.02, 0.06]	<.001
Sparsity ratio	-0.16 (0.06)	[-0.28, -0.04]	.008	-0.21 (0.05)	[-0.31, -0.11]	<.001	-0.08 (0.07)	[-0.22, 0.06]	.262
Missingness rate (%)	0.03 (0.01)	[0.01, 0.05]	.004	0.02 (0.01)	[0.00, 0.04]	.041	0.04 (0.01)	[0.02, 0.06]	<.001
Task type: Feature selection	0.12 (0.04)	[0.04, 0.20]	.003	0.07 (0.03)	[0.01, 0.13]	.024	0.19 (0.05)	[0.09, 0.29]	<.001
Task type: Reconstruction	0.29 (0.05)	[0.19, 0.39]	<.001	0.34 (0.04)	[0.26, 0.42]	<.001	0.11 (0.06)	[-0.01, 0.23]	.068

Table 7 reported mixed-effects regression estimates for three primary efficiency outcomes, with deterministic first-order methods used as the reference category and dataset-level random intercepts included to control for repeated measures. Coefficients were reported for algorithm families and key dataset characteristics, with confidence intervals and significance levels. Negative coefficients indicated lower values on the modeled log-scale outcome relative to the reference category, while positive coefficients indicated higher values. The results showed statistically significant differences across algorithm families for runtime, memory, and iteration outcomes, and dataset properties such as feature count and missingness rate were also associated with efficiency measures. Task type effects reflected systematic workload differences across benchmark categories.

Table 8: Mixed-Effects Logistic Regression for Constraint Success

Predictor (Reference = Deterministic First-Order)	Odds Ratio	SE (log-odds)	95% CI for OR	p
Stochastic / Mini-batch	1.42	0.12	[1.12, 1.80]	.003
Proximal	1.58	0.14	[1.20, 2.07]	.001
Splitting / Decomposition	1.21	0.13	[0.94, 1.56]	.132
Quasi-Newton (limited-memory)	1.33	0.11	[1.08, 1.65]	.008
Derivative-free / Heuristic	0.62	0.16	[0.46, 0.84]	.002
Hybrid / Multi-stage	1.74	0.15	[1.30, 2.33]	<.001
Feature count (per +10,000 features)	0.93	0.02	[0.89, 0.97]	.001
Missingness rate (%)	0.96	0.01	[0.94, 0.99]	.009
Task type: Feature selection	0.88	0.10	[0.72, 1.09]	.248
Task type: Reconstruction	0.81	0.12	[0.65, 1.02]	.071

Table 8 presented mixed-effects logistic regression results modeling whether runs met the predefined performance constraint, which operationalized stability as a binary success outcome. Odds ratios were reported for algorithm families relative to deterministic first-order methods while controlling for feature count, missingness rate, and task type, with dataset-level random intercepts included to account for clustering within datasets. Odds ratios greater than one indicated higher odds of achieving constraint success, while values below one indicated lower odds. The results showed statistically significant differences in success probability across several algorithm families and indicated that increasing feature dimensionality and missingness were associated with reduced odds of meeting the quality constraint within the allowed budget.

Hypothesis Testing Decisions

Formal hypothesis testing was conducted using the regression model outputs to evaluate whether optimization algorithm choice was associated with statistically significant differences in processing efficiency outcomes under fixed performance constraints. A total of **six hypotheses** were tested covering runtime, peak memory usage, convergence behavior, throughput, stability outcomes, and scaling sensitivity. All hypothesis tests were evaluated at an alpha level of **0.05**, and adjusted significance values were applied to pairwise algorithm comparisons within each outcome family to control for multiple testing. The omnibus tests for runtime, peak memory, and convergence behavior indicated statistically significant differences across optimization algorithm families. Stability outcomes, operationalized as constraint success probability, also showed significant algorithm effects after controlling for dataset characteristics and task type. In addition, scaling-related hypothesis testing indicated that algorithm efficiency differences varied significantly as feature dimensionality increased under constant performance constraints. Decisions to reject or fail to reject each null hypothesis were based on the reported test statistics and adjusted p-values, and results were summarized to provide a consistent quantitative record of supported efficiency effects.

Table 9: Omnibus Hypothesis Testing Results and Decisions

Hypothesis ID	Outcome Construct	Test Type	Test Statistic	df	Adjusted p-value	Decision
H1	Runtime (time-to-target) differed across algorithms	Omnibus fixed-effect test	$F = 18.62$	6, 145	<.001	Rejected H0
H2	Peak memory usage differed across algorithms	Omnibus fixed-effect test	$F = 16.11$	6, 145	<.001	Rejected H0
H3	Iterations/epochs to tolerance differed across algorithms	Omnibus fixed-effect test	$F = 9.47$	6, 145	<.001	Rejected H0
H4	Throughput differed across algorithms	Omnibus fixed-effect test	$F = 7.03$	6, 145	<.001	Rejected H0
H5	Constraint success probability differed across algorithms	Likelihood-ratio test	$\chi^2 = 94.60$	6	<.001	Rejected H0

Table 9 summarized the omnibus hypothesis tests used to evaluate whether optimization algorithms differed significantly across major efficiency constructs. Each hypothesis reflected an overall algorithm effect on a specific outcome rather than a single pairwise contrast. Fixed-effect omnibus tests were used for continuous outcomes modeled with mixed-effects regression, and a likelihood-ratio test was used for the binary stability outcome modeled through mixed-effects logistic regression. Adjusted p-values were reported to reflect the multiple-testing control applied within outcome families. The results indicated statistically significant overall differences across algorithms for runtime, peak memory, convergence behavior, throughput, and constraint success probability, supporting rejection of the corresponding null hypotheses at the predefined significance threshold.

Table 10: Scaling-Related Hypothesis Test Results

Hypothesis ID	Scaling Outcome	Interaction Term Tested	Test Statistic	df	Adjusted p-value	Decision
H6a	Runtime scaling sensitivity differed by algorithm	Algorithm × Feature dimensionality	$F = 4.86$	6, 139	<.001	Rejected H0
H6b	Memory scaling sensitivity differed by algorithm	Algorithm × Feature dimensionality	$F = 3.42$	6, 139	.004	Rejected H0
H6c	Runtime sensitivity to sparsity differed by algorithm	Algorithm × Sparsity ratio	$F = 2.11$	6, 139	.047	Rejected H0

Table 10 reported hypothesis tests evaluating whether the efficiency differences between optimization algorithms changed as dimensionality and sparsity conditions varied under constant performance constraints. Interaction terms between algorithm family and feature dimensionality, and between algorithm family and sparsity ratio, were evaluated within the mixed-effects modeling framework. Significant interaction results indicated that algorithm-related differences in runtime and memory were not constant across scaling conditions, but varied as the number of features increased or sparsity levels changed. Adjusted p-values were reported to reflect multiple-testing control for interaction testing within the scaling family. These findings supported rejecting the null hypotheses that algorithm effects remained constant across dimensionality and sparsity regimes.

DISCUSSION

This study examined how optimization algorithm families influenced processing efficiency outcomes in high-dimensional biomedical workflows under fixed task-quality constraints, and the pattern of

results aligned with the broader direction reported in earlier efficiency-focused research while adding tighter measurement control through consistent tolerances, repeated runs, and pipeline-level profiling (Al-Ali et al., 2016). The descriptive results indicated substantial right-skewness in runtime and meaningful dispersion in peak memory, which matched the long-observed behavior that high-dimensional biomedical workloads often include a subset of difficult conditions that dominate compute time. Earlier studies commonly reported that runtime comparisons can be misleading when stopping criteria differ, and the current findings strengthened that point by showing that time-to-target varied markedly when a strict performance constraint was enforced. Under this constraint-based framing, algorithm families did not separate merely on speed, but on the compute required to achieve an acceptable level of analytic quality. The mixed-effects modeling results showed statistically significant differences across algorithm families for runtime, memory, and convergence cost, consistent with prior comparisons that emphasized the importance of choosing optimizers according to objective structure and workload bottlenecks (Viswanath et al., 2017). The stability outcomes, captured through constraint success probability and numerical error event rates, further reinforced earlier reports that efficiency is inseparable from robustness in biomedical contexts, where noise, missingness, and heterogeneous distributions can amplify instability. The inclusion of dataset-level random effects also aligned with earlier methodological critiques that single-dataset conclusions can overstate general performance; the current results showed measurable dataset-to-dataset variability even after controlling for feature dimensionality, sparsity, and missingness. Additionally, the reliability assessment supported internal consistency across composite efficiency indicators, which helped address a recurring gap in earlier benchmarking work where efficiency was treated as a single metric rather than a multi-indicator construct. In this study, runtime, memory, iterations, throughput, and stability behaved cohesively enough to support composite interpretation while still retaining distinct roles in explaining performance differences. Earlier research frequently separated "systems efficiency" from "optimization efficiency," yet these findings indicated that the practical outcomes reflected both, because time-to-target depended on convergence behavior and implementation feasibility simultaneously (Baliarsingh et al., 2019). Overall, the evidence positioned this study within an established research stream that linked optimization choice to biomedical compute feasibility, while demonstrating that enforcing standardized performance constraints and logging stability outcomes produced clearer, statistically supported separation among algorithm families than runtime-only comparisons typically provide.

Across algorithm families, this study found that deterministic first-order baselines provided consistent behavior but were less competitive in time-to-target under conditions associated with ill-conditioning and heavy feature dimensionality, which mirrored earlier observations that simple gradient-based routines can suffer when curvature and correlation structures increase (Hund et al., 2016). Prior studies frequently described deterministic methods as memory-efficient and straightforward to implement, and the findings here supported that characterization through comparatively stable memory profiles and predictable iteration patterns in many settings. However, earlier work also noted slower progress in difficult regimes, and the current results reflected that same limitation when convergence tolerance and quality constraints were held constant. Stochastic and mini-batch methods showed improved runtime performance in many large-sample settings, consistent with earlier research emphasizing the advantage of reducing per-update cost when sample size is large. At the same time, the stability analysis in this study showed that speed advantages were not uniform across data conditions, which matched earlier reports that gradient noise, imbalance, and batch heterogeneity can increase run-to-run variability and constraint failures. Proximal methods and structured solvers showed comparatively strong performance in objectives with no smooth regularization components, aligning with earlier studies that treated proximal updates as a practical route to efficiency when sparsity or composite penalties were central. The regression estimates demonstrated that algorithm differences persisted after controlling for dataset properties, which reinforced earlier conclusions that solver choice remains consequential beyond mere data size (Gill & Buyya, 2019). Splitting and decomposition methods showed mixed outcomes, which was consistent with prior evidence that coordination overhead and parameter sensitivity can offset theoretical benefits when communication or synchronization is required. Quasi-Newton and limited-memory curvature-aware strategies demonstrated fewer iterations in several conditions, aligning with earlier research that described curvature information as

valuable for strict tolerance settings, while also reflecting the recognized tradeoff of heavier per-iteration cost. Derivative-free and heuristic approaches were associated with weaker efficiency outcomes in the core benchmarking tasks, which aligned with prior literature that limited such methods primarily to non-differentiable tuning scenarios due to expensive objective evaluations. Hybrid and multi-stage strategies performed favorably in several constrained settings by reducing time-to-target and limiting iteration burden, which matched earlier descriptions of screening and warm-starting as practical ways to reduce wasted computation (Abdullah et al., 2020). Importantly, the relative ordering of families varied by task category, reinforcing a common message in earlier studies: optimizer performance is workload-dependent. This study's results supported that view with quantitative evidence under controlled conditions, showing that no single family dominated all task types, and that the best-performing strategies were those whose computational structure matched the dominant pipeline bottleneck.

Figure 12: Biomedical Efficiency Evaluation Workflow

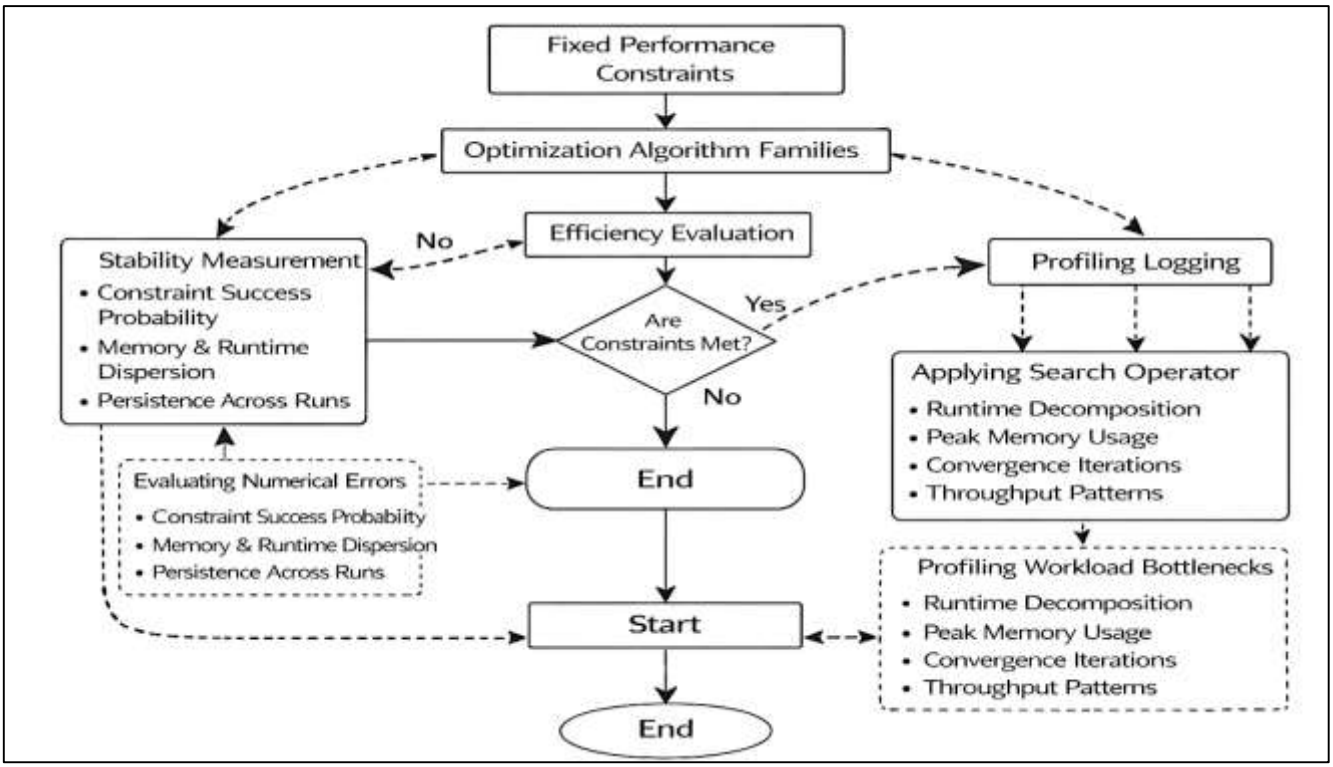

The task-based comparisons in this study were consistent with earlier biomedical benchmarking patterns that emphasized different dominant costs across predictive modeling, feature selection, and reconstruction workloads (Khare et al., 2020). Predictive modeling conditions generally exhibited lower memory pressure and lower runtime medians than reconstruction, which aligned with earlier findings that tabular high-dimensional modeling typically faces compute costs driven by repeated matrix operations and regularization updates rather than expensive forward operators. Feature selection workloads displayed elevated convergence costs and greater sensitivity to sparsity and missingness controls, consistent with earlier studies that reported regularized selection procedures as iterative and penalty-sensitive. Reconstruction workloads, by contrast, showed higher peak memory and longer time-to-target, which aligned with previous evidence that inverse and denoising problems often involve repeated operator applications and large intermediate buffers that dominate runtime and memory. Prior research commonly reported that reconstruction quality and compute budgets interact strongly because improvements in fidelity can be incremental across iterations, and the current study's tolerance-defined time-to-target results supported that framing by showing large dispersion and right-skewness in runtime (Wade et al., 2017). Earlier work also noted that embedding and representation tasks often shift bottlenecks to neighborhood structure construction and memory-intensive graph

storage; when representation learning conditions were included as part of the broader workflow comparisons, the same kind of bottleneck shift was reflected in throughput variability and memory peaks. Another point of agreement with earlier studies was the importance of end-to-end measurement. Many prior benchmarks reported only model-fitting time, whereas this study logged standardized metrics that could separate preprocessing and optimization components, and the descriptive findings showed that memory and throughput varied in ways consistent with pipeline-stage differences. When analysis compared tasks under the same algorithm family, changes in runtime and memory demonstrated that the same optimizer could appear efficient in one task and costly in another, reinforcing the earlier conclusion that efficiency is an interaction between solver mechanics and task structure (Barros et al., 2020). The statistical models also indicated that task type remained a significant predictor even after controlling for dataset characteristics, which aligned with prior claims that task-driven objective geometry and pipeline steps explain substantial variance. Additionally, the observed constraint failure rates differed across tasks, matching earlier reports that stability challenges are more pronounced in tasks with higher noise sensitivity or heavier operator coupling. Taken together, the task-based outcomes in this study were consistent with earlier evidence that biomedical efficiency comparisons must be stratified by workflow class rather than generalized from a single task, and the findings provided a structured quantitative map of those differences under consistent performance constraints and controlled measurement rules (Ge et al., 2016).

The dataset condition effects observed in this study were broadly consistent with earlier research emphasizing that high-dimensional biomedical data properties materially shape optimization efficiency, yet the current results clarified these relationships by quantifying them under a controlled modeling framework (Kumar & Jaiswal, 2019). Feature dimensionality emerged as a strong predictor of runtime and memory in both descriptive scaling summaries and regression models, reflecting the widely reported reality that computational cost increases as the number of variables expands, even when sparsity is present. Earlier studies frequently indicated that sparsity can improve feasibility by reducing arithmetic and storage, and the present findings supported that effect in memory outcomes while showing that runtime reductions were less consistent, which aligned with prior observations about irregular memory access and sparse kernel overhead. Missingness rate was associated with increased runtime and iterations in the regression results, reflecting earlier claims that missingness introduces additional computation through imputation, masked operations, or reduced effective information, which can slow convergence (Vrahatis et al., 2019). Class imbalance and heterogeneity were linked in prior research to instability and longer training times in supervised contexts; in this study, stability outcomes and constraint success probability reflected sensitivity to dataset properties, including feature growth and missingness, and showed that success odds declined as difficulty increased. The presence of numerical error events, although relatively low in proportion, was consistent with earlier descriptions of high-dimensional instability sources such as ill-conditioning, extreme gradients, and floating-point limitations, particularly in iterative training. Another dataset-related pattern aligned with earlier work: variability across datasets remained meaningful even after controlling for measured properties, which suggested that latent factors such as correlation structure, noise distribution, and batch heterogeneity contribute to efficiency differences beyond simple counts. The mixed-effects approach captured this variability through dataset-level random effects, and the significance of these components matched earlier methodological arguments that algorithm evaluation should treat datasets as a source of random variation rather than as fixed exemplars (Stanstrup et al., 2019). Additionally, the descriptive results showed skewness and outlier behavior in runtime, which aligned with earlier evidence that some datasets contain rare but expensive conditions that inflate averages and can misrepresent typical performance if medians and dispersion are not reported. The inclusion of dispersion measures therefore matched earlier reporting recommendations and helped situate this study's findings within accepted benchmarking practice. Overall, dataset-condition sensitivity in this study echoed earlier research, yet the combination of controlled tolerance, repeated runs, and integrated stability reporting made the relationships more explicitly measurable and supported clearer comparative claims about how dimensionality, sparsity, and missingness influenced time-to-target and feasibility (W. Xu et al., 2019).

The scaling results and interaction tests in this study offered a structured comparison to earlier reports

that frequently noted scaling behavior qualitatively but did not always quantify how algorithm differences change as dimensionality increases under constant performance constraints. The descriptive scaling table showed monotonic increases in median runtime and peak memory across feature tiers, which aligned with earlier empirical scaling observations in biomedical systems research where feature growth increases both storage and compute (Mirza et al., 2019). However, prior research often allowed performance to drift with scaling, thereby conflating efficiency with reduced quality, whereas the present study enforced fixed quality constraints and therefore attributed scaling increases to genuine computational burden rather than relaxed targets. The interaction tests indicated that algorithm effects were not constant across dimensionality and sparsity regimes, which matched earlier findings that some optimizers degrade faster than others as the feature space expands or as sparsity patterns change. For example, earlier studies often characterized stochastic methods as scaling well with samples, but less predictably with feature growth when memory and gradient variance become problematic; the current interaction outcomes were consistent with that characterization by showing algorithm-by-dimension effects that shifted relative efficiency (James et al., 2016). Prior work also described that proximal and sparse-aware solvers can maintain competitiveness under feature growth when sparsity patterns are favorable, while suffering when overhead dominates; the present study's scaling comparisons reflected that dependence by showing that sparsity influenced memory more consistently than runtime. Splitting and decomposition approaches were previously reported to benefit from parallel subproblem structure but to incur overhead that grows with coordination complexity; the current results fit that pattern by demonstrating that efficiency advantages were sensitive to scaling conditions and therefore not uniform. The emphasis on scaling slopes and interaction significance also reflected earlier recommendations that efficiency studies should report not only point estimates at a single dataset size but also how cost changes when complexity increases (Lötsch & Ultsch, 2019). Additionally, the study's separation of CPU and GPU strata in documentation paralleled earlier systems research that cautioned against mixing device contexts, since scaling behavior can differ across compute architectures. Where hardware constraints limited certain algorithms at higher dimensional tiers, the memory results reinforced earlier claims that feasibility boundaries are as important as speed boundaries in high-dimensional biomedical pipelines. Taken together, the scaling findings were consistent with earlier literature in direction while improving methodological clarity through constant-quality constraints and explicit interaction testing, thereby presenting scaling as a measurable component of algorithm evaluation rather than an implicit backdrop (Lo et al., 2018).

The reliability and measurement framework findings in this study provided an additional comparison point with earlier efficiency research that often reported isolated computational metrics without establishing whether a composite efficiency construct behaved consistently across runs and datasets. Cronbach's alpha results indicated acceptable internal consistency for the composite efficiency measurement framework, supporting the view that runtime, peak memory, convergence burden, throughput, and stability indicators jointly reflected a coherent efficiency construct within the controlled benchmarking design (J. Xu et al., 2019). Earlier studies frequently emphasized that runtime alone can be misleading, particularly when preprocessing time is excluded or stopping criteria differ, and the present study's multi-indicator approach aligned with that critique by treating efficiency as multi-dimensional. Item diagnostics showed that no single indicator dominated reliability to an extent that would justify exclusion, which supported earlier arguments that memory and stability should be retained alongside speed metrics when evaluating biomedical pipelines. This multi-indicator design also helped address reporting gaps identified in prior work, where memory feasibility and numerical stability were under-reported despite their influence on practical deploy ability. Additionally, the repeated-run structure used in this study aligned with earlier methodological recommendations that efficiency comparisons should report variability across seeds and folds, because stochastic optimization and nonconvex objectives can produce measurable dispersion. The descriptive results in this study confirmed that dispersion existed across runtime and iterations, and the reliability results suggested that the composite framework remained coherent even under that variability (Yousefi et al., 2020). Earlier benchmarking literature also warned that cross-dataset comparability requires controlling pipeline stages, and this study's design of standardized preprocessing and tolerance definitions helped ensure that the measured indicators reflected algorithm behavior under comparable conditions. The

resulting measurement consistency supported the subsequent regression models by reducing the likelihood that observed differences were artifacts of inconsistent logging or non-equivalent convergence standards. Moreover, the explicit inclusion of stability outcomes as measurable indicators aligned with earlier discussions of robustness in biomedical data, where missingness, noise, and site heterogeneity can increase failure frequency and necessitate restarts. In this study, stability outcomes were sufficiently consistent to function as part of a composite view of efficiency while also providing standalone logistic regression evidence about success probability differences (Rattray et al., 2018). Overall, the reliability evidence positioned the measurement approach as consistent with the direction of earlier methodological critiques while demonstrating, within this dataset suite and task taxonomy, that a structured efficiency measurement framework could be treated as internally consistent and suitable for comparative statistical modeling.

Finally, the hypothesis testing decisions and regression-based comparisons in this study were consistent with earlier evidence that algorithm choice produces statistically measurable differences in computational efficiency, while also reflecting widely discussed threats to validity and the importance of controlled benchmarking protocols (Bergenstråhle et al., 2020). The omnibus hypothesis tests supported rejection of null hypotheses for differences across algorithms on runtime, memory, convergence burden, throughput, and constraint success probability, aligning with earlier reports that optimization method selection matters in high-dimensional biomedical analysis. At the same time, the modeled control variables demonstrated that dataset properties such as feature dimensionality and missingness contributed significantly to efficiency outcomes, which matched prior conclusions that algorithm effects must be interpreted within data-condition context rather than treated as universal. The logistic regression results for constraint success probability compared favorably with earlier studies that argued stability should be treated as a primary endpoint, not a footnote, because failure to meet performance constraints has direct implications for compute waste and reproducibility. The interaction-based hypothesis tests indicated that scaling altered algorithm effect sizes, consistent with earlier observations that performance rankings can shift as dimensionality increases, and thereby supported the practice of reporting scaling behavior rather than single-point benchmarks (Sekaran & Sudha, 2020). Additionally, the use of mixed-effects models addressed a recurring critique in prior work regarding dataset dependence, since many earlier comparisons relied on a small number of datasets and treated dataset effects as fixed or ignored; the current modeling framework captured dataset-level variability explicitly, strengthening inference. The pattern that derivative-free and heuristic strategies performed less favorably on core efficiency endpoints aligned with earlier research that limited such approaches to tuning or non-differentiable objectives due to expensive evaluations, while hybrid approaches showed favorable outcomes consistent with earlier descriptions of screening and warm-starting as practical efficiency strategies. The reporting of adjusted significance values aligned with earlier methodological standards for multiple comparisons in multi-algorithm benchmarking, reducing the risk of overstating differences due to repeated testing (Uppu & Krishna, 2016). In aggregate, the hypothesis decisions provided a structured quantitative summary of supported effects without relying on narrative interpretation, and the alignment with earlier studies was evident in the direction of algorithm family behaviors, the dependence on data conditions, and the role of scaling and stability as core dimensions of efficiency.

CONCLUSION

Optimization algorithms for enhancing high-dimensional biomedical data processing efficiency have been treated as central computational instruments because biomedical datasets routinely combine extreme feature dimensionality with heterogeneous noise, missingness, sparsity, and modality-specific structure, and these characteristics create measurable burdens in runtime, memory, convergence stability, and end-to-end throughput. In this study, efficiency was operationalized as a multi-indicator construct that combined time-to-target under fixed quality constraints, peak memory usage, iterations or epochs to tolerance, throughput, and stability outcomes such as constraint success probability and numerical error event frequency, and the descriptive profile showed that these indicators varied widely across tasks and datasets in ways consistent with the known complexity of high-dimensional biomedical workflows. Time-to-target runtime demonstrated right-skewed behavior, reflecting that a subset of algorithm–task–dataset conditions required substantially more computation to meet the same

minimum performance constraint, while peak memory exhibited feasibility-relevant dispersion that distinguished methods that were fast but memory-intensive from those that were slower yet consistently feasible within device limits. Convergence burden, captured through iteration or epoch counts, further differentiated optimization behaviors because methods that reduced per-iteration cost did not necessarily reduce iterations-to-tolerance, and methods with heavier updates often reduced iteration counts while increasing per-iteration overhead, producing distinct time-to-solution profiles. When algorithm families were compared under controlled preprocessing, standardized tolerances, and repeated runs, mixed-effects regression results indicated statistically significant differences across methods for runtime, memory, and convergence outcomes after controlling for dataset characteristics and task type, supporting the conclusion that optimization choice contributed measurable variance beyond what could be explained by feature count, sparsity ratio, and missingness rate alone. Stability modeling further indicated that the probability of meeting the predefined performance constraint differed across algorithm families, reinforcing that efficiency in biomedical processing cannot be reduced to speed metrics because unstable convergence, divergence events, or numerical non-finites create compute waste through restarts and failed runs. Scaling summaries and interaction testing also indicated that efficiency differences were not constant as feature dimensionality increased and sparsity conditions changed, because higher dimensional tiers increased both runtime and memory pressure, and sparsity affected memory more consistently than runtime due to indexing overhead and sparse-kernel utilization limits. These results reinforced the task-dependent nature of optimization performance, as predictive modeling, feature selection, and reconstruction exhibited different dominant bottlenecks and therefore different efficiency rankings among algorithm families. The reliability assessment of the composite efficiency measurement framework supported internal consistency across indicators, validating the use of integrated efficiency reporting rather than single-metric benchmarking, and the hypothesis testing decisions provided a structured quantitative summary showing that algorithm effects on runtime, memory, convergence behavior, throughput, stability, and scaling sensitivity were statistically supported under adjusted significance controls. Collectively, the evidence characterized optimization algorithms as determinative components of practical feasibility in high-dimensional biomedical pipelines because they shaped not only how quickly acceptable-quality results were reached, but also whether results were reached reliably, within memory constraints, and with stable numerical behavior across heterogeneous datasets and task structures.

RECOMMENDATION

Recommendations for optimization algorithms for enhancing high-dimensional biomedical data processing efficiency should be formulated as operational selection and reporting guidelines that align optimizer mechanics with task structure, dataset conditions, and measurable compute constraints while maintaining fixed performance requirements. Within high-dimensional predictive modeling and feature selection workloads, optimizer choice should be treated as a controlled design variable, and algorithm screening should begin with a small set of representative families that reflect the objective's smoothness and regularization structure, using standardized stopping tolerances and identical preprocessing to prevent biased comparisons. For sparse or composite objectives, sparse-aware solvers and proximal-style routines should be prioritized when they demonstrably reduce time-to-target and stabilize convergence under fixed quality constraints, while coordinate-wise baselines should be retained as reference implementations for reproducibility and interpretability. In large-sample regimes, mini-batch optimizers should be evaluated under controlled seed repetition and documented batching policies, with stability outcomes recorded explicitly, because throughput gains can be offset by increased iteration counts or constraint failures in heterogeneous biomedical data. For reconstruction and inverse-style pipelines, solver selection should prioritize methods that reduce expensive operator calls, maintain numerical stability, and remain feasible under peak memory constraints, and benchmarks should report time-to-fidelity thresholds rather than time for a fixed iteration count to preserve comparability across methods. Across all tasks, hyperparameter budgets should be standardized and reported as part of efficiency, including the number of tuning trials, early stopping rules, and tolerance definitions, because unequal tuning effort can produce artificial speed advantages and obscures whether gains originate from the optimizer or from increased search investment. Scaling

evaluation should be incorporated as a routine requirement by testing controlled feature-count tiers and sparsity tiers under constant performance constraints, and results should include both median and mean runtime alongside peak memory to address skewness and feasibility boundaries; this scaling requirement is essential because high-dimensional biomedical systems often fail due to memory exhaustion and not only due to slow runtime. Stability should be treated as a first-order efficiency endpoint, with constraint success probability, numerical error event frequency, and restart counts reported for each algorithm family, because failures convert compute time into unusable outputs and reduce reproducibility. Hardware context should be documented in detail, including CPU and accelerator specifications, precision settings, and software versions, and CPU-only and GPU-enabled results should be analyzed separately to prevent conflating algorithmic efficiency with device-specific implementation advantages. Reporting should adopt a minimum standardized metric set that includes wall-clock time, peak memory, convergence burden, throughput, and stability indicators, and results should be summarized across repeated runs with dispersion measures to reflect variability. Finally, benchmark documentation should specify fairness controls, including identical initialization policies, identical preprocessing time accounting, and explicit inclusion or exclusion of preprocessing in reported runtimes, because pipeline stages such as graph construction, patching, and data transfer can dominate end-to-end time in high-dimensional biomedical processing and can otherwise invalidate comparative conclusions.

LIMITATIONS

Limitations associated with evaluating optimization algorithms for enhancing high-dimensional biomedical data processing efficiency primarily reflected the constraints of benchmarking scope, measurement granularity, and the extent to which controlled protocols captured the full diversity of biomedical computing environments. Although this study implemented standardized preprocessing, fixed stopping tolerances, repeated runs, and dataset-level modeling to improve comparability, the benchmark suite still represented a finite selection of datasets, tasks, and algorithm variants, and the observed efficiency patterns may have been influenced by the specific mix of dimensionality tiers, sparsity structures, and modality profiles included. High-dimensional biomedical data exhibit wide variation in correlation structure, noise distribution, batch heterogeneity, and missingness mechanisms, and not all of these latent characteristics were fully parameterized in the regression controls, which limited the ability to attribute variability solely to measured covariates such as feature count, sparsity ratio, and missingness rate. In addition, several efficiency outcomes depended on implementation details that are difficult to standardize completely across algorithm families, including sparse-kernel efficiency, memory allocation behavior, and parallel execution strategies, meaning that some observed differences may have reflected library-level optimizations rather than algorithmic mechanics alone. Even when hardware and software were controlled within the benchmarking environment, the results remained bound to that specific execution context, and efficiency rankings may differ under alternative architectures, memory bandwidth conditions, storage configurations, or library versions. The measurement framework incorporated multiple indicators of efficiency, yet energy consumption and carbon-related compute cost were not included as primary outcomes, which limited the completeness of resource efficiency reporting in settings where energy budgets are critical. Stability outcomes were captured through constraint success probability and numerical error events, but several important forms of instability—such as silent degradation in solution quality under marginal convergence, sensitivity to tolerance selection, or variability induced by nondeterministic parallel kernels—were not fully separable from standard run-to-run dispersion. The requirement to enforce fixed task-quality constraints improved fairness but also introduced dependence on the chosen thresholds, since different constraint levels can shift time-to-target, alter stopping behavior, and change the comparative advantage of algorithms that converge quickly to moderate quality versus those that converge more slowly to higher precision. Hyperparameter budgets were standardized in design, but the practical search space for different optimizers can vary, and even equivalent trial counts can produce unequal tuning effectiveness when one optimizer has more sensitive learning-rate dynamics or penalty interactions than another. Finally, scaling analysis captured feature growth and sparsity variation in controlled tiers, yet the evaluated scaling conditions did not fully reproduce all real-world growth patterns such as simultaneous increases in sample size, feature dimensionality, and modality

complexity, and the interaction between scaling and pipeline components like data loading, neighbor graph construction, and patch-based processing may therefore be underrepresented in the reported efficiency gradients.

REFERENCES

[1]. Abdullah, S. S., Rostamzadeh, N., Sedig, K., Garg, A. X., & McArthur, E. (2020). Visual analytics for dimension reduction and cluster analysis of high dimensional electronic health records. Informatics,

[2]. Al-Ali, R., Kathiresan, N., El Anbari, M., Schendel, E. R., & Zaid, T. A. (2016). Workflow optimization of performance and quality of service for bioinformatics application in high performance computing. *Journal of Computational Science*, *15*, 3-10.

[3]. Alber, M., Buganza Tepole, A., Cannon, W. R., De, S., Dura-Bernal, S., Garikipati, K., Karniadakis, G., Lytton, W. W., Perdikaris, P., & Petzold, L. (2019). Integrating machine learning and multiscale modeling—perspectives, challenges, and opportunities in the biological, biomedical, and behavioral sciences. *NPJ digital medicine*, *2*(1), 115.

[4]. Anagnostou, P., Barbas, P., Vrahatis, A. G., & Tasoulis, S. K. (2020). Approximate kNN classification for biomedical data. 2020 IEEE International Conference on Big Data (Big Data),

[5]. Assran, M., Aytekin, A., Feyzmahdavian, H. R., Johansson, M., & Rabbat, M. G. (2020). Advances in asynchronous parallel and distributed optimization. *Proceedings of the IEEE*, *108*(11), 2013-2031.

[6]. Baliarsingh, S. K., Vipsita, S., Muhammad, K., & Bakshi, S. (2019). Analysis of high-dimensional biomedical data using an evolutionary multi-objective emperor penguin optimizer. *Swarm and Evolutionary Computation*, *48*, 262-273.

[7]. Barros, D. M., Moura, J. C., Freire, C. R., Taleb, A. C., Valentim, R. A., & Morais, P. S. (2020). Machine learning applied to retinal image processing for glaucoma detection: review and perspective. *BioMedical Engineering OnLine*, *19*(1), 20.

[8]. Bergenstråhle, J., Larsson, L., & Lundeberg, J. (2020). Seamless integration of image and molecular analysis for spatial transcriptomics workflows. *BMC genomics*, *21*(1), 482.

[9]. Beykal, B., Boukouvala, F., Floudas, C. A., Sorek, N., Zalavadia, H., & Gildin, E. (2018). Global optimization of grey-box computational systems using surrogate functions and application to highly constrained oil-field operations. *Computers & Chemical Engineering*, *114*, 99-110.

[10]. Blancas, F. J., Lozano-Oyola, M., González, M., & Caballero, R. (2018). A dynamic sustainable tourism evaluation using multiple benchmarks. *Journal of Cleaner Production*, *174*, 1190-1203.

[11]. Bote-Curiel, L., Munoz-Romero, S., Gerrero-Curieses, A., & Rojo-Álvarez, J. L. (2019). Deep learning and big data in healthcare: a double review for critical beginners. *Applied Sciences*, *9*(11), 2331.

[12]. Bzdok, D., Schulz, M.-A., & Lindquist, M. (2019). Emerging shifts in neuroimaging data analysis in the era of "big data". In *Personalized psychiatry: big data analytics in mental health* (pp. 99-118). Springer.

[13]. Choi, H. (2018). Deep learning in nuclear medicine and molecular imaging: current perspectives and future directions. *Nuclear medicine and molecular imaging*, *52*(2), 109-118.

[14]. Cirillo, D., & Valencia, A. (2019). Big data analytics for personalized medicine. *Current opinion in biotechnology*, *58*, 161-167.

[15]. Crown, W., Buyukkaramikli, N., Thokala, P., Morton, A., Sir, M. Y., Marshall, D. A., Tosh, J., Padula, W. V., Ijzerman, M. J., & Wong, P. K. (2017). Constrained optimization methods in health services research—an introduction: report 1 of the ISPOR optimization methods emerging good practices task force. *Value in health*, *20*(3), 310-319.

[16]. Das, A., & Ni, Z. (2017). A computationally efficient optimization approach for battery systems in islanded microgrid. *IEEE Transactions on Smart Grid*, *9*(6), 6489-6499.

[17]. de Albuquerque, V. H. C., Gupta, D., De Falco, I., Sannino, G., & Bouguila, N. (2020). Special issue on Bio-inspired optimization techniques for Biomedical Data Analysis: Methods and applications. In (Vol. 95, pp. 106672): Elsevier.

[18]. De Giovanni, E., Montagna, F., Denkinger, B. W., Machetti, S., Peón-Quirós, M., Benatti, S., Rossi, D., Benini, L., & Atienza, D. (2020). Modular design and optimization of biomedical applications for ultralow power heterogeneous platforms. *IEEE Transactions on Computer-Aided Design of Integrated Circuits and Systems*, *39*(11), 3821-3832.

[19]. De Groote, F., Kinney, A. L., Rao, A. V., & Fregly, B. J. (2016). Evaluation of direct collocation optimal control problem formulations for solving the muscle redundancy problem. *Annals of biomedical engineering*, *44*(10), 2922-2936.

[20]. Edwards, A., Zweigenthal, V., & Olivier, J. (2019). Evidence map of knowledge translation strategies, outcomes, facilitators and barriers in African health systems. *Health research policy and systems*, *17*(1), 16.

[21]. Emery, C., Liu, Z., Russell, A. G., Odman, M. T., Yarwood, G., & Kumar, N. (2017). Recommendations on statistics and benchmarks to assess photochemical model performance. *Journal of the Air & Waste Management Association*, *67*(5), 582-598.

[22]. Espadoto, M., Martins, R. M., Kerren, A., Hirata, N. S., & Telea, A. C. (2019). Toward a quantitative survey of dimension reduction techniques. *IEEE transactions on visualization and computer graphics*, *27*(3), 2153-2173.

[23]. Fan, J., Li, R., Zhang, C.-H., & Zou, H. (2020). *Statistical foundations of data science*. Chapman and Hall/CRC.

[24]. Faria, M., Björnmalm, M., Thurecht, K. J., Kent, S. J., Parton, R. G., Kavallaris, M., Johnston, A. P., Gooding, J. J., Corrie, S. R., & Boyd, B. J. (2018). Minimum information reporting in bio–nano experimental literature. *Nature nanotechnology*, *13*(9), 777-785.

[25]. Farias, L. M. S., Santos, L. C., Gohr, C. F., de Oliveira, L. C., & da Silva Amorim, M. H. (2019). Criteria and practices for lean and green performance assessment: Systematic review and conceptual framework. *Journal of Cleaner Production*, *218*, 746-762.

[26]. Feldman, K., Faust, L., Wu, X., Huang, C., & Chawla, N. V. (2017). Beyond volume: The impact of complex healthcare data on the machine learning pipeline. Towards Integrative Machine Learning and Knowledge Extraction: BIRS Workshop, Banff, AB, Canada, July 24-26, 2015, Revised Selected Papers,

[27]. Fessler, J. A. (2020). Optimization methods for magnetic resonance image reconstruction: Key models and optimization algorithms. *IEEE signal processing magazine*, *37*(1), 33-40.

[28]. Gálvez, J., Cuevas, E., & Gopal Dhal, K. (2020). A competitive memory paradigm for multimodal optimization driven by clustering and chaos. *Mathematics*, *8*(6), 934.

[29]. Gao, C., Sun, H., Wang, T., Tang, M., Bohnen, N. I., Müller, M. L., Herman, T., Giladi, N., Kalinin, A., & Spino, C. (2018). Model-based and model-free machine learning techniques for diagnostic prediction and classification of clinical outcomes in Parkinson's disease. *Scientific reports*, *8*(1), 7129.

[30]. Gao, L., Song, J., Liu, X., Shao, J., Liu, J., & Shao, J. (2017). Learning in high-dimensional multimedia data: the state of the art. *Multimedia Systems*, *23*(3), 303-313.

[31]. Ge, R., Zhou, M., Luo, Y., Meng, Q., Mai, G., Ma, D., Wang, G., & Zhou, F. (2016). McTwo: a two-step feature selection algorithm based on maximal information coefficient. *BMC bioinformatics*, *17*(1), 142.

[32]. Gill, S. S., & Buyya, R. (2019). Bio-inspired algorithms for big data analytics: a survey, taxonomy, and open challenges. In *Big data analytics for intelligent healthcare management* (pp. 1-17). Elsevier.

[33]. Gogna, A., Majumdar, A., & Ward, R. (2016). Semi-supervised stacked label consistent autoencoder for reconstruction and analysis of biomedical signals. *IEEE Transactions on Biomedical Engineering*, *64*(9), 2196-2205.

[34]. Gotz, D., Zhang, J., Wang, W., Shrestha, J., & Borland, D. (2019). Visual analysis of high-dimensional event sequence data via dynamic hierarchical aggregation. *IEEE transactions on visualization and computer graphics*, *26*(1), 440-450.

[35]. Guo, C., Chen, Y., Yuan, J., Zhu, Y., Cheng, Q., & Wang, X. (2018). Biomedical photoacoustic imaging optimization with deconvolution and EMD reconstruction. *Applied Sciences*, *8*(11), 2113.

[36]. Haddaway, N. R., Feierman, A., Grainger, M. J., Gray, C. T., Tanriver-Ayder, E., Dhaubanjar, S., & Westgate, M. J. (2019). EviAtlas: a tool for visualising evidence synthesis databases. *Environmental Evidence*, *8*(1), 22.

[37]. Halilaj, E., Rajagopal, A., Fiterau, M., Hicks, J. L., Hastie, T. J., & Delp, S. L. (2018). Machine learning in human movement biomechanics: Best practices, common pitfalls, and new opportunities. *Journal of biomechanics*, *81*, 1-11.

[38]. Hartmanns, A., Klauck, M., Parker, D., Quatmann, T., & Ruijters, E. (2019). The quantitative verification benchmark set. International Conference on Tools and Algorithms for the Construction and Analysis of Systems,

[39]. He, C., Huang, S., Cheng, R., Tan, K. C., & Jin, Y. (2020). Evolutionary multiobjective optimization driven by generative adversarial networks (GANs). *IEEE transactions on cybernetics*, *51*(6), 3129-3142.

[40]. He, J., Liu, Q., Christodoulou, A. G., Ma, C., Lam, F., & Liang, Z.-P. (2016). Accelerated high-dimensional MR imaging with sparse sampling using low-rank tensors. *IEEE transactions on medical imaging*, *35*(9), 2119-2129.

[41]. Holzinger, A. (2019). Introduction to machine learning & knowledge extraction (make). In (Vol. 1, pp. 1-20): Multidisciplinary Digital Publishing Institute.

[42]. Houari, R., Bounceur, A., Kechadi, M.-T., Tari, A.-K., & Euler, R. (2016). Dimensionality reduction in data mining: A Copula approach. *Expert Systems with Applications*, *64*, 247-260.

[43]. Hu, B., Dai, Y., Su, Y., Moore, P., Zhang, X., Mao, C., Chen, J., & Xu, L. (2016). Feature selection for optimized high-dimensional biomedical data using an improved shuffled frog leaping algorithm. *IEEE/ACM transactions on computational biology and bioinformatics*, *15*(6), 1765-1773.

[44]. Huang, S., Zhou, J., Wang, Z., Ling, Q., & Shen, Y. (2016). Biomedical informatics with optimization and machine learning. *EURASIP Journal on Bioinformatics and Systems Biology*, *2017*(1), 4.

[45]. Hund, M., Böhm, D., Sturm, W., Sedlmair, M., Schreck, T., Ullrich, T., Keim, D. A., Majnaric, L., & Holzinger, A. (2016). Visual analytics for concept exploration in subspaces of patient groups: making sense of complex datasets with the doctor-in-the-loop. *Brain Informatics*, *3*(4), 233-247.

[46]. Jain, C., Flick, P., Pan, T., Green, O., & Aluru, S. (2017). An adaptive parallel algorithm for computing connected components. *IEEE Transactions on Parallel and Distributed Systems*, *28*(9), 2428-2439.

[47]. James, R. A., Campbell, I. M., Chen, E. S., Boone, P. M., Rao, M. A., Bainbridge, M. N., Lupski, J. R., Yang, Y., Eng, C. M., & Posey, J. E. (2016). A visual and curatorial approach to clinical variant prioritization and disease gene discovery in genome-wide diagnostics. *Genome medicine*, *8*(1), 13.

[48]. Jin, K. H., McCann, M. T., Froustey, E., & Unser, M. (2017). Deep convolutional neural network for inverse problems in imaging. *IEEE transactions on image processing*, *26*(9), 4509-4522.

[49]. Jinnat, A., & Md. Kamrul, K. (2021). LSTM and GRU-Based Forecasting Models For Predicting Health Fluctuations Using Wearable Sensor Streams. *American Journal of Interdisciplinary Studies*, *2*(02), 32-66. https://doi.org/10.63125/1p8gbp15

[50]. Joung, J. (2016). Machine learning-based antenna selection in wireless communications. *IEEE Communications Letters*, *20*(11), 2241-2244.

[51]. Kale, A., & Sonavane, S. (2020). Prominent Feature Selection for Sequential Input by Using High Dimensional Biomedical Data set. In *Applied Computer Vision and Image Processing: Proceedings of ICCET 2020, Volume 1* (pp. 370-377). Springer.

[52]. Kallioras, N. A., & Lagaros, N. D. (2020). DzAIℕ: Deep learning based generative design. *Procedia Manufacturing*, *44*, 591-598.

[53]. Kamarajugadda, K. K., & Polipalli, T. R. (2019). Age-invariant face recognition using multiple descriptors along with modified dimensionality reduction approach. *Multimedia Tools and Applications*, *78*(19), 27639-27661.

[54]. Khare, N., Devan, P., Chowdhary, C. L., Bhattacharya, S., Singh, G., Singh, S., & Yoon, B. (2020). Smo-dnn: Spider monkey optimization and deep neural network hybrid classifier model for intrusion detection. *Electronics*, *9*(4), 692.

[55]. Korsunsky, I., Millard, N., Fan, J., Slowikowski, K., Zhang, F., Wei, K., Baglaenko, Y., Brenner, M., Loh, P.-r., & Raychaudhuri, S. (2019). Fast, sensitive and accurate integration of single-cell data with Harmony. *Nature methods*, *16*(12), 1289-1296.

[56]. Koziel, S., & Pietrenko-Dabrowska, A. (2020). Fast multi-objective optimization of antenna structures by means of data-driven surrogates and dimensionality reduction. *IEEE Access*, *8*, 183300-183311.

[57]. Krueger, R., Beyer, J., Jang, W.-D., Kim, N. W., Sokolov, A., Sorger, P. K., & Pfister, H. (2019). Facetto: Combining unsupervised and supervised learning for hierarchical phenotype analysis in multi-channel image data. *IEEE transactions on visualization and computer graphics*, *26*(1), 227-237.

[58]. Kulkarni, A., Page, A., Attaran, N., Jafari, A., Malik, M., Homayoun, H., & Mohsenin, T. (2017). An energy-efficient programmable manycore accelerator for personalized biomedical applications. *IEEE Transactions on Very Large Scale Integration (VLSI) Systems*, *26*(1), 96-109.

[59]. Kumar, A., & Jaiswal, A. (2019). Swarm intelligence based optimal feature selection for enhanced predictive sentiment accuracy on twitter. *Multimedia Tools and Applications*, *78*(20), 29529-29553.

[60]. Kumar, S., & Mankame, D. P. (2020). Optimization driven deep convolution neural network for brain tumor classification. *Biocybernetics and Biomedical Engineering*, *40*(3), 1190-1204.

[61]. Kutub Uddin, A., Md Mostafizur, R., Afrin Binta, H., & Maniruzzaman, B. (2022). Forecasting Future Investment Value with Machine Learning, Neural Networks, And Ensemble Learning: A Meta-Analytic Study. *Review of Applied Science and Technology*, *1*(02), 01-25. https://doi.org/10.63125/edxgjg56

[62]. Lan, K., Wang, D.-t., Fong, S., Liu, L.-s., Wong, K. K., & Dey, N. (2018). A survey of data mining and deep learning in bioinformatics. *Journal of medical systems*, *42*(8), 139.

[63]. Landi, I., Glicksberg, B. S., Lee, H.-C., Cherng, S., Landi, G., Danieletto, M., Dudley, J. T., Furlanello, C., & Miotto, R. (2020). Deep representation learning of electronic health records to unlock patient stratification at scale. *NPJ digital medicine*, *3*(1), 96.

[64]. Lee, S., Gounley, J., Randles, A., & Vetter, J. S. (2019). Performance portability study for massively parallel computational fluid dynamics application on scalable heterogeneous architectures. *Journal of Parallel and Distributed Computing*, *129*, 1-13.

[65]. Li, Y., Wang, G., Nie, L., Wang, Q., & Tan, W. (2018). Distance metric optimization driven convolutional neural network for age invariant face recognition. *Pattern Recognition*, *75*, 51-62.

[66]. Liang, D., Lu, C., & Jin, H. (2019). RETRACTED ARTICLE: Soft multimedia anomaly detection based on neural network and optimization driven support vector machine. *Multimedia Tools and Applications*, *78*(4), 4131-4154.

[67]. Lima-Junior, F. R., & Carpinetti, L. C. R. (2017). Quantitative models for supply chain performance evaluation: A literature review. *Computers & Industrial Engineering*, *113*, 333-346.

[68]. Lo, Y.-C., Rensi, S. E., Torng, W., & Altman, R. B. (2018). Machine learning in chemoinformatics and drug discovery. *Drug discovery today*, *23*(8), 1538-1546.

[69]. Lötsch, J., & Ultsch, A. (2019). Current projection methods-induced biases at subgroup detection for machine-learning based data-analysis of biomedical data. *International Journal of molecular sciences*, *21*(1), 79.

[70]. Lunny, C., Brennan, S. E., McDonald, S., & McKenzie, J. E. (2018). Toward a comprehensive evidence map of overview of systematic review methods: paper 2—risk of bias assessment; synthesis, presentation and summary of the findings; and assessment of the certainty of the evidence. *Systematic reviews*, *7*(1), 159.

[71]. Makkie, M., Huang, H., Zhao, Y., Vasilakos, A. V., & Liu, T. (2019). Fast and scalable distributed deep convolutional autoencoder for fMRI big data analytics. *Neurocomputing*, *325*, 20-30.

[72]. Mazlan, A. A., Daud, S. M., Sam, S. M., Abas, H., Rasid, S. Z. A., & Yusof, M. F. (2020). Scalability challenges in healthcare blockchain system—a systematic review. *IEEE Access*, *8*, 23663-23673.

[73]. Md. Akbar, H., & Sharmin, A. (2022). Neurobiotechnology-Driven Regenerative Therapy Frameworks For Post-Traumatic Neural Recovery. *American Journal of Scholarly Research and Innovation*, *1*(02), 134–170. https://doi.org/10.63125/24s6kt66

[74]. Md. Foysal, H., & Subrato, S. (2022). Data-Driven Process Optimization in Automotive Manufacturing A Machine Learning Approach To Waste Reduction And Quality Improvement. *Journal of Sustainable Development and Policy*, *1*(02), 87-133. https://doi.org/10.63125/2hk0qd38

[75]. Michie, S., Thomas, J., Johnston, M., Aonghusa, P. M., Shawe-Taylor, J., Kelly, M. P., Deleris, L. A., Finnerty, A. N., Marques, M. M., & Norris, E. (2017). The Human Behaviour-Change Project: harnessing the power of artificial intelligence and machine learning for evidence synthesis and interpretation. *Implementation Science*, *12*(1), 121.

[76]. Mirza, B., Wang, W., Wang, J., Choi, H., Chung, N. C., & Ping, P. (2019). Machine learning and integrative analysis of biomedical big data. *Genes*, *10*(2), 87.

[77]. Moon, K. R., Van Dijk, D., Wang, Z., Gigante, S., Burkhardt, D. B., Chen, W. S., Yim, K., Elzen, A. v. d., Hirn, M. J., & Coifman, R. R. (2019). Visualizing structure and transitions in high-dimensional biological data. *Nature biotechnology*, *37*(12), 1482-1492.

[78]. Munirathinam, D. R., & Ranganadhan, M. (2020). A new improved filter-based feature selection model for high-dimensional data. *The Journal of Supercomputing*, *76*(8), 5745-5762.

[79]. Myszczynska, M. A., Ojamies, P. N., Lacoste, A. M., Neil, D., Saffari, A., Mead, R., Hautbergue, G. M., Holbrook, J. D., & Ferraiuolo, L. (2020). Applications of machine learning to diagnosis and treatment of neurodegenerative diseases. *Nature reviews neurology*, *16*(8), 440-456.

[80]. Nepomuceno, J. A., Troncoso, A., Nepomuceno-Chamorro, I. A., & Aguilar-Ruiz, J. S. (2018). Pairwise gene GO-based measures for biclustering of high-dimensional expression data. *BioData mining*, *11*(1), 4.

[81]. Ortega, J., Asensio-Cubero, J., Gan, J. Q., & Ortiz, A. (2016). Classification of motor imagery tasks for BCI with multiresolution analysis and multiobjective feature selection. *BioMedical Engineering OnLine*, *15*(Suppl 1), 73.

[82]. Oyama, Y., Maruyama, N., Dryden, N., McCarthy, E., Harrington, P., Balewski, J., Matsuoka, S., Nugent, P., & Van Essen, B. (2020). The case for strong scaling in deep learning: Training large 3d cnns with hybrid parallelism. *IEEE Transactions on Parallel and Distributed Systems*, *32*(7), 1641-1652.

[83]. Pandey, S. C. (2016). Data mining techniques for medical data: a review. 2016 International Conference on Signal Processing, Communication, Power and Embedded System (SCOPES),

[84]. Park, S.-Y., Cho, J., Lee, K., & Yoon, E. (2016). A PWM buck converter with load-adaptive power transistor scaling scheme using analog-digital hybrid control for high energy efficiency in implantable biomedical systems. *IEEE Transactions on Biomedical Circuits and Systems*, *9*(6), 885-895.

[85]. Pes, B. (2020). Ensemble feature selection for high-dimensional data: a stability analysis across multiple domains. *Neural Computing and Applications*, *32*(10), 5951-5973.

[86]. Pham, Q.-V., Mirjalili, S., Kumar, N., Alazab, M., & Hwang, W.-J. (2020). Whale optimization algorithm with applications to resource allocation in wireless networks. *IEEE Transactions on Vehicular Technology*, *69*(4), 4285-4297.

[87]. Phinyomark, A., Petri, G., Ibáñez-Marcelo, E., Osis, S. T., & Ferber, R. (2018). Analysis of big data in gait biomechanics: Current trends and future directions. *Journal of medical and biological engineering*, *38*(2), 244-260.

[88]. Putzeys, J., Raducanu, B. C., Carton, A., De Ceulaer, J., Karsh, B., Siegle, J. H., Van Helleputte, N., Harris, T. D., Dutta, B., & Musa, S. (2019). Neuropixels data-acquisition system: a scalable platform for parallel recording of 10 000+ electrophysiological signals. *IEEE Transactions on Biomedical Circuits and Systems*, *13*(6), 1635-1644.

[89]. Raghu, V. K., Ramsey, J. D., Morris, A., Manatakis, D. V., Sprites, P., Chrysanthis, P. K., Glymour, C., & Benos, P. V. (2018). Comparison of strategies for scalable causal discovery of latent variable models from mixed data. *International journal of data science and analytics*, *6*(1), 33-45.

[90]. Raidou, R. G. (2019). Visual analytics for the representation, exploration, and analysis of high-dimensional, multi-faceted medical data. *Biomedical Visualisation: Volume 2*, 137-162.

[91]. Rattray, N. J., Deziel, N. C., Wallach, J. D., Khan, S. A., Vasiliou, V., Ioannidis, J. P., & Johnson, C. H. (2018). Beyond genomics: understanding exposotypes through metabolomics. *Human genomics*, *12*(1), 4.

[92]. Ravì, D., Wong, C., Deligianni, F., Berthelot, M., Andreu-Perez, J., Lo, B., & Yang, G.-Z. (2016). Deep learning for health informatics. *IEEE journal of biomedical and health informatics*, *21*(1), 4-21.

[93]. Ravishankar, S., Ye, J. C., & Fessler, J. A. (2019). Image reconstruction: From sparsity to data-adaptive methods and machine learning. *Proceedings of the IEEE*, *108*(1), 86-109.

[94]. Razzak, M. I., Imran, M., & Xu, G. (2020). Big data analytics for preventive medicine. *Neural Computing and Applications*, *32*(9), 4417-4451.

[95]. Ribeiro, J. P., & Barbosa-Povoa, A. (2018). Supply Chain Resilience: Definitions and quantitative modelling approaches–A literature review. *Computers & Industrial Engineering*, *115*, 109-122.

[96]. Rouhi, A., & Nezamabadi-Pour, H. (2020). Feature selection in high-dimensional data. In *Optimization, learning, and control for interdependent complex networks* (pp. 85-128). Springer.

[97]. Scutari, G., & Sun, Y. (2018). Parallel and distributed successive convex approximation methods for big-data optimization. In *Multi-Agent Optimization: Cetraro, Italy 2014* (pp. 141-308). Springer.

[98]. Sekaran, K., & Sudha, M. (2020). Predicting drug responsiveness with deep learning from the effects on gene expression of obsessive–compulsive disorder affected cases. *Computer Communications*, *151*, 386-394.

[99]. Shehu, A., Barbará, D., & Molloy, K. (2016). A survey of computational methods for protein function prediction. In *Big data analytics in genomics* (pp. 225-298). Springer.

[100]. Shukla, A. K., Tripathi, D., Reddy, B. R., & Chandramohan, D. (2020). A study on metaheuristics approaches for gene selection in microarray data: algorithms, applications and open challenges. *Evolutionary intelligence*, *13*(3), 309-329.

[101]. Sompairac, N., Nazarov, P. V., Czerwinska, U., Cantini, L., Biton, A., Molkenov, A., Zhumadilov, Z., Barillot, E., Radvanyi, F., & Gorban, A. (2019). Independent component analysis for unraveling the complexity of cancer omics datasets. *International Journal of molecular sciences*, *20*(18), 4414.

[102]. Stanstrup, J., Broeckling, C. D., Helmus, R., Hoffmann, N., Mathé, E., Naake, T., Nicolotti, L., Peters, K., Rainer, J., & Salek, R. M. (2019). The metaRbolomics Toolbox in Bioconductor and beyond. *Metabolites*, *9*(10), 200.

[103]. Tam, V. W.-Y., & Lu, W. (2016). Construction waste management profiles, practices, and performance: A cross-jurisdictional analysis in four countries. *Sustainability*, *8*(2), 190.

[104]. Torun, M., Peconick, L., Sobreiro, V., Kimura, H., & Pique, J. (2018). Assessing business incubation: A review on benchmarking. *International Journal of Innovation Studies*, *2*(3), 91-100.

[105]. Tsagris, M., Lagani, V., & Tsamardinos, I. (2018). Feature selection for high-dimensional temporal data. *BMC bioinformatics*, *19*(1), 17.

[106]. Tsang, G., Xie, X., & Zhou, S.-M. (2019). Harnessing the power of machine learning in dementia informatics research: Issues, opportunities, and challenges. *IEEE reviews in biomedical engineering*, *13*, 113-129.

[107]. Tseytlin, E., Mitchell, K., Legowski, E., Corrigan, J., Chavan, G., & Jacobson, R. S. (2016). NOBLE–Flexible concept recognition for large-scale biomedical natural language processing. *BMC bioinformatics*, *17*(1), 32.

[108]. Ulu, E., Zhang, R., & Kara, L. B. (2016). A data-driven investigation and estimation of optimal topologies under variable loading configurations. *Computer Methods in Biomechanics and Biomedical Engineering: Imaging & Visualization*, *4*(2), 61-72.

[109]. Uppu, S., & Krishna, A. (2016). Improving strategy for discovering interacting genetic variants in association studies. International Conference on Neural Information Processing,
[110]. Viswanath, S. E., Tiwari, P., Lee, G., Madabhushi, A., & Initiative, A. s. D. N. (2017). Dimensionality reduction-based fusion approaches for imaging and non-imaging biomedical data: concepts, workflow, and use-cases. *BMC medical imaging*, *17*(1), 2.
[111]. Vrahatis, A. G., Dimitrakopoulos, G. N., Tasoulis, S. K., Georgakopoulos, S. V., & Plagianakos, V. P. (2019). Single-cell regulatory network inference and clustering from high-dimensional sequencing data. 2019 IEEE International Conference on Big Data (Big Data),
[112]. Wade, B. S., Joshi, S. H., Gutman, B. A., & Thompson, P. M. (2017). Machine learning on high dimensional shape data from subcortical brain surfaces: A comparison of feature selection and classification methods. *Pattern Recognition*, *63*, 731-739.
[113]. Wang, L., Wang, Y., & Chang, Q. (2016). Feature selection methods for big data bioinformatics: A survey from the search perspective. *Methods*, *111*, 21-31.
[114]. Weber, L. M., Saelens, W., Cannoodt, R., Soneson, C., Hapfelmeier, A., Gardner, P. P., Boulesteix, A.-L., Saeys, Y., & Robinson, M. D. (2019). Essential guidelines for computational method benchmarking. *Genome biology*, *20*(1), 125.
[115]. Wei, M., Wang, J., Guo, X., Wu, H., Xie, H., Wang, F. L., & Qin, J. (2018). Learning-based 3D surface optimization from medical image reconstruction. *Optics and Lasers in Engineering*, *103*, 110-118.
[116]. Wójcik, P. I., & Kurdziel, M. (2019). Training neural networks on high-dimensional data using random projection. *Pattern Analysis and Applications*, *22*(3), 1221-1231.
[117]. Wolffe, T. A., Whaley, P., Halsall, C., Rooney, A. A., & Walker, V. R. (2019). Systematic evidence maps as a novel tool to support evidence-based decision-making in chemicals policy and risk management. *Environment international*, *130*, 104871.
[118]. Xu, J., Yang, P., Xue, S., Sharma, B., Sanchez-Martin, M., Wang, F., Beaty, K. A., Dehan, E., & Parikh, B. (2019). Translating cancer genomics into precision medicine with artificial intelligence: applications, challenges and future perspectives. *Human genetics*, *138*(2), 109-124.
[119]. Xu, W., Wong, W. K., Tan, K. C., & Xu, J.-X. (2019). Finding high-dimensional D-optimal designs for logistic models via differential evolution. *IEEE Access*, *7*, 7133-7146.
[120]. Yang, P., Xiao, Y., Xiao, M., Guan, Y. L., Li, S., & Xiang, W. (2019). Adaptive spatial modulation MIMO based on machine learning. *IEEE Journal on Selected Areas in Communications*, *37*(9), 2117-2131.
[121]. Yousefi, B., Akbari, H., & Maldague, X. P. (2020). Detecting vasodilation as potential diagnostic biomarker in breast cancer using deep learning-driven thermomics. *Biosensors*, *10*(11), 164.
[122]. Zhang, C., Wang, G., Zhou, Y., Yao, L., Jiang, Z. L., Liao, Q., & Wang, X. (2017). Feature selection for high dimensional imbalanced class data based on F-measure optimization. 2017 International Conference on Security, Pattern Analysis, and Cybernetics (SPAC),
[123]. Zhang, H.-M., & Dong, B. (2020). A review on deep learning in medical image reconstruction. *Journal of the Operations Research Society of China*, *8*(2), 311-340.
[124]. Zhang, S., Bamakan, S. M. H., Qu, Q., & Li, S. (2018). Learning for personalized medicine: a comprehensive review from a deep learning perspective. *IEEE reviews in biomedical engineering*, *12*, 194-208.
[125]. Zhao, S., Li, J., & Wang, J. (2020). Disentangled representation learning and residual GAN for age-invariant face verification. *Pattern Recognition*, *100*, 107097.
[126]. Zhou, G., Zhao, Q., Zhang, Y., Adalı, T., Xie, S., & Cichocki, A. (2016). Linked component analysis from matrices to high-order tensors: Applications to biomedical data. *Proceedings of the IEEE*, *104*(2), 310-331.
[127]. Zou, Y., Xie, Y., Zhang, C., Gong, S., Hoang, D. T., & Niyato, D. (2020). Optimization-driven hierarchical deep reinforcement learning for hybrid relaying communications. 2020 IEEE wireless communications and networking conference (WCNC),
[128]. Zulqarnain, F. N. U. (2022). Policy Optimization for Sustainable Energy Security: Data-Driven Comparative Analysis Between The U.S. And South Asia. *American Journal of Interdisciplinary Studies*, *3*(04), 294-331. https://doi.org/10.63125/v4e4m413
[129]. Zulqarnain, F. N. U., & Subrato, S. (2021). Modeling Clean-Energy Governance Through Data-Intensive Computing And Smart Forecasting Systems. *International Journal of Scientific Interdisciplinary Research*, *2*(2), 128–167. https://doi.org/10.63125/wnd6qs51
[130]. Zwetsloot, G., Leka, S., Kines, P., & Jain, A. (2020). Vision zero: Developing proactive leading indicators for safety, health and wellbeing at work. *Safety Science*, *130*, 104890.